Bioscene

Bioscene
Volume- 21 Number- 04
ISSN: 1539-2422 (P) 2055-1583 (O)
www.explorebioscene.com

Comparative Studies of Cerium Oxideusing Green and Chemical Synthesis on Biological and Photo Catalytic Applications as Reactive free Radical Species: A review

Anuj Kumar[1],Anita Bisht[2], Ajay Singh[3],Manisha[4], Sarvesh Kumar[5], Ritu Vishnoi[6],Navneet Swami[7],Payal Verma[7], Peeush Singhal[8]

Corresponding Author: **Dr. Peeush Singhal**

Abstract: Cerium oxide nanoparticles (CeO_2 NPs) have garnered significant attention due to their unique redox properties, making them promising candidates for various biological and photocatalytic applications, particularly in mitigating reactive free radical species. This review provides a comprehensive comparison of CeO_2 NPs synthesized via green and chemical methods, focusing on their efficiency and effectiveness in biological and photocatalytic applications. Green synthesis, utilizing plant extracts, microorganisms, and other eco-friendly resources, is emerging as a sustainable alternative to traditional chemical synthesis. This method not only reduces environmental impact but also imparts unique properties to the nanoparticles, such as enhanced biocompatibility and reduced toxicity. On the other hand, chemical synthesis methods, while offering precise control over particle size and morphology, often involve hazardous chemicals and energy-intensive processes, which may limit their applicability in environmentally sensitive areas. The review examines the role of CeO_2 NPs in scavenging reactive oxygen species (ROS) and reactive nitrogen species (RNS) in biological systems, highlighting their potential in therapeutic applications such as neuroprotection, anti-inflammatory treatments, and cancer therapy. Additionally, the photocatalytic properties of CeO_2 NPs are analyzed, particularly in environmental remediation processes like water purification and pollutant degradation. Through a comparative analysis, the review aims to elucidate the advantages and limitations of both synthesis approaches, providing insights into their practical applications and future prospects in combating reactive free radical species. The findings suggest that while green synthesis holds promise for safer and more sustainable production of CeO_2 NPs, further research is needed to optimize their properties and expand their applications in both biological and environmental contexts.

Key Words: Cerium Oxide, Green and Chemical Synthesis, Photocatalytic Applications, reactive free radical

Introduction

Metal oxide nanoparticles are the most popular and have an important role in applications in diverse fieldssuch as medicine [1], imaging [2], energy storage[3],

fuel cell, and catalyst[4]to nanomedicine. Metal oxide nanomaterials enhance theproperties of bulk materials and molecules and driving force for the development of new technologies for the future.The variousproperties of nanomaterials are related to the increase in the surface area to volume of nanoparticles that affects the physiochemical properties that cause the new attractive applications such as UV absorption ability [5], UV emitters [6] phosphors [7][8], solid electrolytes and electrochromic devices[9], cool LEDs [10], Solid oxide fuel for a lithium-ion battery[11],supercapacitor [12],solid lubricants [13],solar cells [14].In the last twenty years, metal oxide nanoparticles (NPs) have had potential applications in wastewater treatment as they showed higher toxicity against ordinary heterotrophic organisms, anaerobic, and ammonia-oxidizing bacteria and hence used for environmental protection[15].

Cerium (Ce) is one of the mostimportant n-type semiconductor metals and high abundance naturally occurring of lanthanide series in the periodic. Cerium rare-earth metal in the Earth's crust.Ceriumis malleable,soft, and ductile in nature. Cerium has its unique electronic configuration [Xe]-$4f^1$,$5d^1 6s^2$.The energy of the inner 4f level is almost equal to the energy of the valence electron[16].Cerium oxide materials have cubic-fluorite-typeoxidewithF_{2g}symmetry and oxygen vacancy [17].Cerium oxideof nanoscale can exist in redox Ce^{+3}/Ce^{+4} sites into their 4f shell of ions and has been an important material and applied in various applications as polishingagents[18], sunscreen[19][20],panthenol stabilized cerium oxide NPs used as cosmeticpurpose as to protect cells under oxidative stressby UV radiation[21],UV shielding materials[22],[23],automatic exhaust catalytic[24],[25],gas sensors[26], humidity sensors [27,28,29], xylene sensors [30],ZnO–CeO_2 nanocompositeasglucose sensor[31], selectively controlled shape ceria nanorods are effective chemical sensors[32].The nanowire structure of ceria acts as a Gas sensor for CO gas [33].Green synthesized cerium oxide with neem oil is used as biofuel[34].

Cerium oxide nanomaterials are also used in biotechnological applications as luminescence bio probes and contrast agents for X-ray computed tomography[35],antimicrobial therapies[36],and antibacterial and antioxidant properties [37].Ceria is widely used as a semiconducting material because of its large band gap energy of 3.14 eV and excitation binding energy. In materials fields applicationsto develop luminescent materials and ionic conductors[38],opticaldevices [39],cerium oxide-coated carbon microspheres capable of enhancing the catalytic ozonation activity[40], and industrial applications [6].Nickle-doped ceria used magnetic data storage devices [41],used as anti-corrosion coating materials due to the super hydrophobicity, UV-resistance, low-cost industrial applications [42],durability, and corrosion resistance[43],solid oxide fuel cell [44].The colloidal cerium oxide nanoparticles showed anticorrosion activity on the aluminiumalloy [45]. The nanoceria actas photocatalysts to degradeRhodamine B (RhB) dye as water pollutants [46].Sensing properties like enzymatic mimics [47],and the food packaging industry[17].rGO-

CeO_2 nanocomposite is used as an excellent photocatalyst for the dye degradation capacity. It degrades90 % of MB dye due to the small bandgap [48].Rosalia Cuahtecontzi-Delint et al 2012 prepared CeO_2 nanoparticles using surfactants to enhance the antibacterial activity twenty times against E. coli [49].

The nanomaterials can be divided into different classes according to their dimensional namely 0D,1D,2D, and 3D.Highly symmetric isotropic spheres,cubes,decahedra, and tetrahedra are classified as 0D nanostructures.They have an important role in nanoscience and nanotechnology.Rods, cylinders,wires, and tubes are examples of 1D nanostructures. Discs,ribbons, and plates with polygon shapesbelong to 2D nanostructures [50].Nanoceria is of different shapes likenanospheres [51],nanorods [52], and controlled synthesis of nanorods by solvothermal using ethylenediamine (40-50 nm diameter and 0.3-2 μm in length) [39], nanowires [53],nanoneedles [54].

In recent years various methods have been developed to improve the physiochemical and biomedical properties of the nanoceria.Some of the important ones are the wet chemical method[55], hydrothermal method[56],[57] a citric acid-mediated hydrothermal method[58], homogenous precipitation method[59],[60], sonochemical method[61,62] a mechanochemical method[63], a composite-hydroxide method[64], Oleate-mediated nanoceria of uniform-size, monodispersed with size 5-20 nm showed strong violet/blue photoluminescent emission at 400 nm [65]. Self-assemblysystem[66],solvent deficient synthesis[67].The various methods of synthesis of ceria were hydroxide-mediated precipitation methods.The prepared sample hasa crystalline of size 9-16 nm,face-centeredcubic, fluorite structure,and nanosphere of 18-30.4 nm size with an absorption peakat 325 nm in biomedical as neurotoxicity[68]. Ammonium acetate mediated chemical precipitation,prepared to nanowires and nanoneedles [54].MonodisperseCeO_2 nanoparticles synthesized by homogenous precipitation method in an alcohol/water solvent mixture[59].Ultrafine single crystalline(size less than 6 nm)CeO_2 nanoparticles witha 100 % productivity ratio using composite hydroxide molten method[64].CeO_2-PA TFN membrane nanocompositeprepared throughthe polymerization methodis used forwater treatment[69].

The reactive free radicalspecies are those species that are very reactive such as oxygen,nitrogen,sulfur, and chloride. These species produce oxidative stress in the cell that results in damage to the protein,lipids,DNA, and the electron transport system of the cell. These species also have an advantage in the degradation of organic pollutants like organic dyes, and hazardous chemicals into less carcinogenic compounds.These free radical species have both beneficial and adverse activity. The beneficial activity islike the biological activity against bacterial,fungal,and viral infections.The anticancer activity and antioxidant activity wereobserved by the nanoceria due to the production of the free radical species. In this review paper, we are going to discuss the comparative studyofthe

physiochemical properties of nanoceriathrough chemical and green methods of synthesis. In the second part how, the physiochemical properties affected the reactive and unstable free radical species in nanoceria and showed biologicaland photocatalytic activity.

1.Chemical Method of Synthesis

The development of cerium oxide nanoparticles has been accomplished chemically in a variety of ways.Some methods were to prepare nanoceria by various chemical methods likeCo-precipitation,sonochemical synthesis, hydrothermal crystallization, microemulsion, microwave, thermal decomposition, spray pyrolysis, sol-gel method,solvothermal synthesis,etc.

1.1.The wet chemical method-The wet chemical synthesis is also known as the solution process.In this method of synthesis,various metal nanomaterials with controllable sizes,shapes,and physiochemical properties were synthesizedthe functional qualities of the nanoparticles,optical, electrical, catalytic, magnetic, etc.are affected by their morphological, structural, and chemical characteristics, which were controlled during the nanomaterials formation.Au nanoparticles are loaded on the ceria nanorod surface through a wet chemical process. $NaBH_4$is used asa reducing agent,and the NPs have higher catalytic activity for the CO oxidation process than CeO_2NPs [70].This method is used to prepare CeO_2 NPs using $CeCl_2.5H_2O$ in HCl medium and ethanol in water(1:1)ratio by volume. After that two solutions are mixed dropwise with continuous stirring, to maintain the pH at 2.Thenthe precipitate was at 70 °C for 4 h,calcined the productwas at 600°C and 1000°C for 4 h.XRD, SEM, TEM, FTIR, and UV-vis techniques were used for characterization.The crystalline phase was cubic fluorite,with increasing temperature it changes to cubic-like with less agglomerate.TEM images showed nanospheres of 20nm size.CeO_2nano sample observeda strong absorption peak in the UV-vis region at the 380 nm rangewith a direct band gap was 3.26 eV [58]. In another study, the CNP'scatalytic properties were modulated with the anion of the precursor salts. The physicalproperties and surface chemistrywere affected by the anions of the precursors duringsynthesisby the wet chemical method in the presence of H_2O_2. The prepared nanoceria has excellent SOD-mimetic activities and antioxidant properties [71].

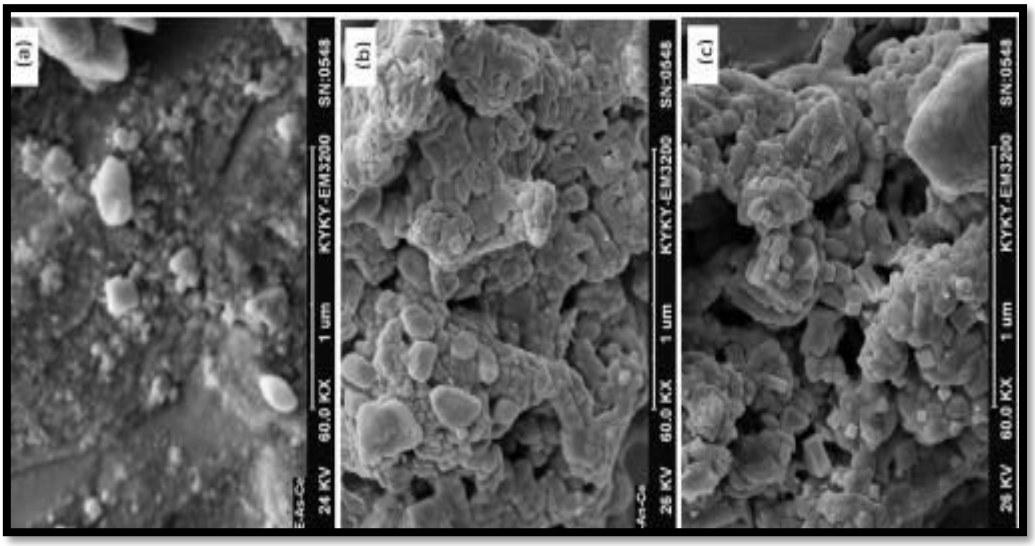

(a)(b)(c)

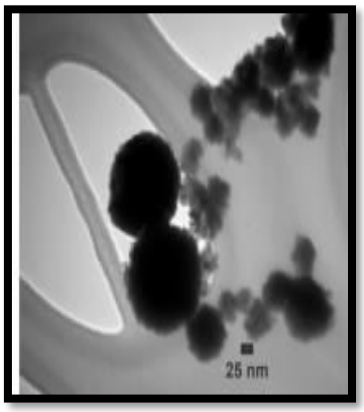

(d)

Figures -1-a,b,c are SEM images of the CeO_2 nanoparticles prepared bythe Wet chemical method.

Figure-1d- is a TEM image of theCeO_2nanoparticlesprepared bythe Wet chemical method.Reference [58].Copyright 2016Hanyang University Press

1.2.The hydrothermal method-Hydrothermal method is one of the most effective methods for the synthesis of metals-basednanomaterials, the most cost-effective,facile,and extensively used route for the synthesis. Wei Wang et al (2010) synthesize the tunable morphologies of ceria nanomaterials of nanorods(5-10

nm),nanowires(40 diameters,length-3-10 μm),and nanospheres(12 nm),without using template and surfactant.In their study, they demonstrated that changing the precursor ions and their concentration affects the morphologies of the products.The precursor Cl^-ions define the nanowirewhileNO_3^-ions tune to the nanospheres.The replacementof the $Cl^-$by PO_4^{-3}ions changes the morphology and shape from nanowires to nanorods[72].The differentmorphology and sizes of ceria nanoparticles were prepared by usingsurfactants such as CTAB,and SDS,andcappingagentslike PVP in the same concentration using a hydroxide mediate hydrothermal approach.The particles of size 40-100 nm were formed using SEM images [73].Rongrong Cui et al. (2009) created a spherical CeO_2 nanostructure by using trisodium citrate dihydrate as a shape controller for the fabrication of 3D-nanoflakes via a simple hydrothermal process that did not require the use of a templet. The temperature and reaction time affected the size, surface morphology, and crystalline nature of the nanostructure. Because of the high surface area BET surfaceof $24m^2/g$, the products formed at 200 °C for 24 h act as a very good oxidative catalyst for CO combustion[74].Abbas et al. (2016) prepared CeO_2 nanostructured microspheres with homogenous multilayers of anaverage size of 40 nm using citric acid. The prepared sample from the hydrothermal method was a nanosheetthathas thepresence of oxygen vacancy than the untreated sample.The nanosheet has very good antibacterial properties due to the oxygen vacancy on the surface of the sample with the bandgap energy was 3.12 eV[75].Shama Sehar et al. 2020 prepared two-shaped nanoceriaby using the hydrothermal method.The precursor cerium nitrate with a mixture of oleic acid,*tert*-butylamine, and toluene wasused for the synthesis.The solution isthen autoclaved at two different temperatures 180°Cand 200 °C respectively.The nanoparticlessynthesizedat 180°Cwere spherical in shapeand Cubical shaped at 200 °C[76]. Spherical-shaped nanoceria was prepared by facile and hard template-free hydrothermal method. The morphology of the prepared nanoceria wascontrolled by using various surfactants.Both types of nanosphere have excellent UV absorption capacity so they are used as ultraviolet shielding materials[22].Similarly, the citric-based nanoceria of size 3.1 nm was prepared by hydrothermal method.The citric acid acts as a protective agent and inhibits theagglomeration of nanoparticles with an average size of 3.1 nm[5].The nanoceria was prepared from the combustion method using different fuels like urea,glycine, glucose, and citric acid.The nature of fuel affects the crystalline and morphology of the sample.The sample prepared from urea is used as anticorrosion pigments while other fuels are used for the inhibitor reservoirs due to high the porosity[77].T. Divya et alin this study characterized that the hydrothermally prepared nanoceria showed more crystalline with cubic structure and Ce+3 species with high oxygen defects that enhance the oxygen storage capacity[78].Zirconium-doped cerium oxide nanomaterials(3 % and 5 % doping of Zr) prepared by hydrothermal method. The particle size is in the 10-15 nm range with a smooth, random, non-uniform distribution of particles from the SAM

image[8].The hydrothermal preparation of (1D)CeO_2NPs of differentsizes, morphology,structure, and optical properties depends on theconc. of NaOH,temperature,and time of synthesis. The nanotubes of nanoceria of different ranges of 5-29,12-36,12-38,and13-59 nm at different times of 6,12,24,48, and72 hof synthesis.The best conditions for the formation of nanotubes were10M NaOH, 125 °C,72 h,concentration,temperature, and timerespectivelyof reaction togivethe highest yield. That makes the ceria nanotubes an excellent photocatalytic properties under visible radiation[89].Formaldehyde-assisted hydrothermal method of preparation 1D nanoceria nanorods ofcrystalline size of 21 -27 nmrange.The nanoceria has very good humidity sensing propertiesas excellent reusable (11-97 %) with very fast response(5 sec)towards the humidity[29].

Figure 2- SEM images of (a) undoped CeO_2(b) 2mol % Gd (c) 8mol % Gd doped CeO_2 nanoparticles. Prepared hydrothermallyRef [81]. Copyright 2017Oriental Scientific Publishing Company

1.3. Chemical precipitation methods: Al-dopednanomaterials of ceria have been prepared by precipitation method using chloride salts of respective metals and ammonia as precursors. The samplecharacterization was done by XRD,SEM, TEM, and DRS.The particle formed size was 6-20 nm.The band gap of the doped nanostructures was decreased with the doping concentration of Aldue to theirsize[82]. The nanoceria was prepared by the precipitation method usingprecursor materialssuch as cerium nitrate and ammonia and using the stream of O_2 and N_2 gas. The reaction pH, temperature, and atmosphere affect the shape and morphology of the nanoparticles.The average size of the particles was increased by increasing the temperature and decreasing theoxygen amount,and the morphology of the particle was altered from square to hexagonal.Above 50% concentration, the forms are a mix of hexagonal and needle-shaped.The bandgap energy increases with the decreasing size of nanoparticles[60]. The doping of iron on cerium oxide nanomaterials affects the size of nanoparticles. The band gap energies of both direct and indirect decreases and lattice parameters increase with the increase in the concentration of iron[83].In the presence of CTAB surfactants, the Fe-loaded nanoceriawas prepared by the co-precipitation method. The TEM images showed the average diameterof the Fe-loaded nanoceria was about 50 nm with uniform and less agglomeration[84]. Quantum-size (4-5 nm)

nanoceria of spherical shapewas prepared by a simple homogenous ammonia precipitation method[85]. Recently the nanoceria were prepared by a simple and cost-effective method co-precipitation method using cationic surfactants CATB.TEM image showed the average particle size of 15.39 nm and oriented in (111) plane.The band gap of the sample was 2.47 eV which indicates the presence of oxygen defects and the presence of Ce^{+3} ion on the surface. The prepared sample dose (0.1-0.7 g/L) showed degradation of MB under UV radiation was 76 % and anticancer activity [86].Zn-doped cerium oxideprepared through the co-precipitation method using oxalic acid as a reducing agent can be a promising nanomaterial for many optoelectronic applications such as solar cells, supercapacitors, sensors, and UV shielding devices[87].

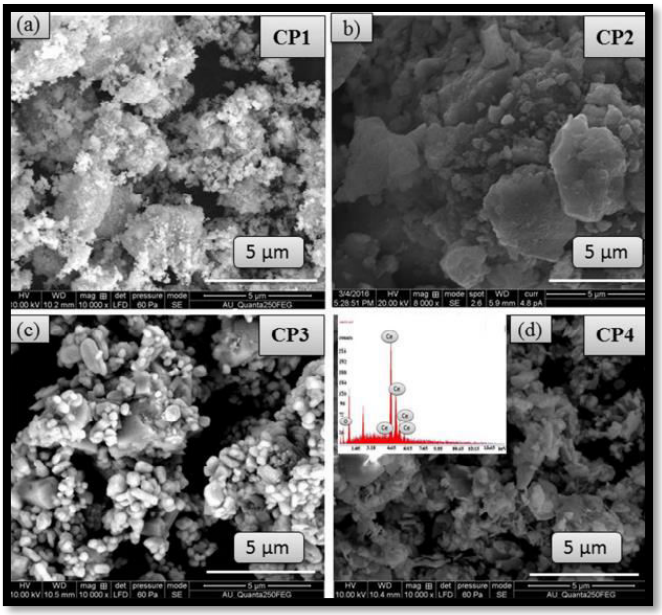

Figure.3-The SEM nanoparticles prepared by co-precipitation method of varying pH as a) 9(CP1), b)10(CP2), c) 11(CP3), and d) 12 (CP4) (Inset: EDX spectra of CP4).Reference [88]. Copyright2019 Elsevier

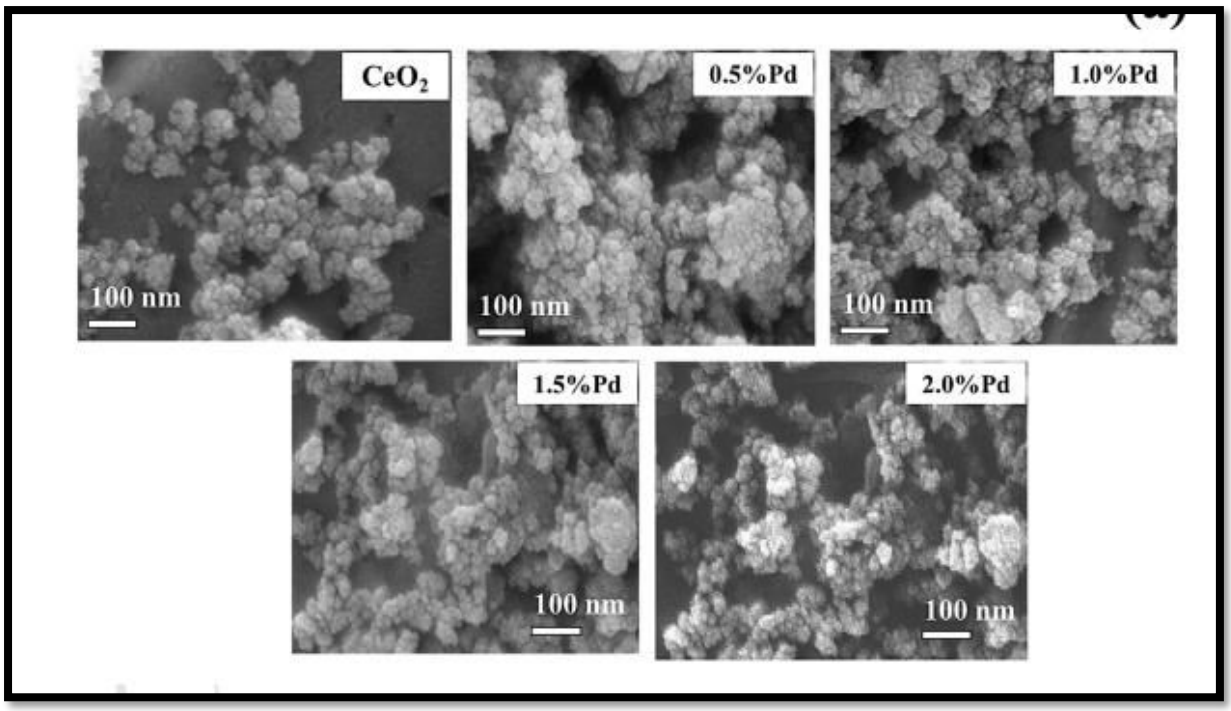

Figure 4-FESEM micrographs of CeO_2 and different percentages of Pd–doped CeO_2 nanoparticles using homogenous ppt methodRef [89]. Copyright 2018 Elsevier

1.4. Microwave synthesis: Siba Soren et al 2015 synthesized the nanoceria by microwave-mediated hydrothermal and microwave-mediated solvothermal methods CeO_2 nanoparticles were synthesized by polyol-mediatedmicrowave method using different precursor salts of Cerium.The formation of nanomaterials within 10 min.XRD pattern showed the cubic crystalline and TEM,SEM images showed agglomeration and particle size wasabout 8-10 nm. The particles formed through the solvothermal method were less agglomerated with smaller sizes between 5 to 10 nm [90].Similarly, the use of NaOH at 12 pH was maintained at 50 ^{C} for 30 minutes heating a microwave. Annealing the product at 800°C for h.The spherical-shaped nanoparticlesof size were around 20 nmwith some agglomerationobserved from SEM and TEM images.Thebandgap was 3.22 eV which is larger than the bulk phase due to the quantum confinementand the UV-vis absorption spectrashowed a strong peak at 321 nm was good agreement according to the size of the nanoparticles [91]

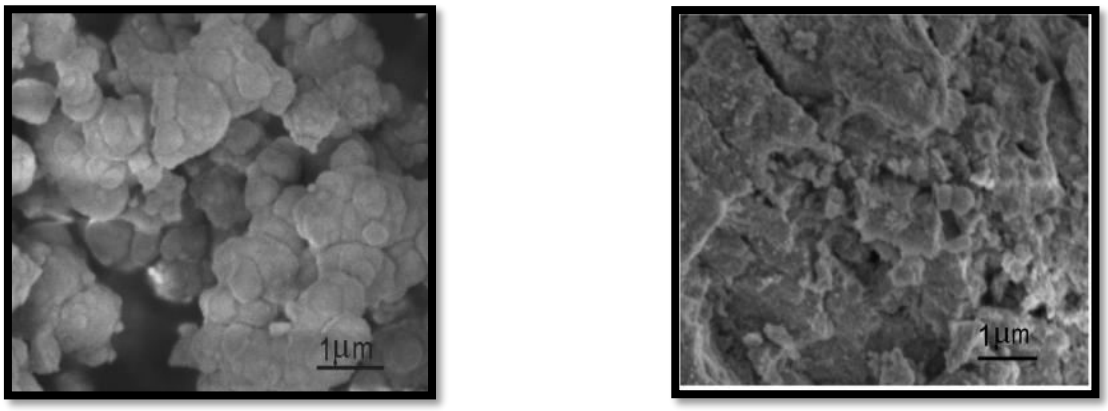

a b

Fig-5a)-Scanning electron micrograph image of CeO_2 synthesized from $(NH_4)_2Ce(NO_3)_6$.

Fig5-b) Scanning electron micrograph image of CeO_2 synthesized from $Ce(NO_3)_3.6H_2O$

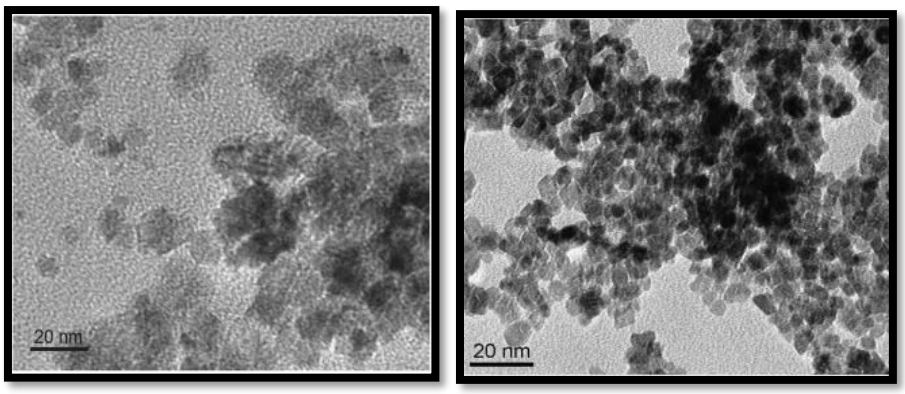

c d

Fig.5-c) Transmission electron micrograph image of CeO_2 synthesized from $(NH_4)_2Ce(NO_3)_6$.

Fig.5-(d) Transmission electron micrograph image of CeO_2 synthesized from$Ce(NO_3)_3.6H_2O$.

Ref [90]. Copyright 2015 Elsevier

2.Green Methods of Synthesis: Green synthesis is derived as the formation of nanostructured by using plant parts extract or microbial like algae,fungus, etc. The methods are highly safe, economical, andenvironmentally friendly as they don't produce any harmful by-products.S.Parvathy and B.R.Venkatraman (2017)synthesized the transition metals doped nano ceria from leaf extract of *Azadirachta Indica*.The structure, surface morphology, and elemental composition were determinedby the XRD,SEM,TEM, and EDAX techniques[92].This study proved that the mycogenesis synthesis of cerium oxide nanoparticleshasa cubic

fluorite structure that is spherical at 5 nm in size and exhibits antibacterial and larvicidal activity against pathogenic bacteria and dengue vectors [93].Spherical-shapedmultifunctionalnanoparticles of CeO_2 were developed by using*Leucas aspera* leaf extract.Theprepared nanoparticles of cubic fluorite structurewith slightly higher lattice constant than the bulk counterpartsbecause ofincreased oxygen vacancies.CeO_2NPs showed superior properties of photocatalytic activity against RhB dye and antibacterial activity against *E.coli* and *S.aureus* bacteria with the zone of inhibition was 4.67 and 3.33 mm respectively.These properties are mainly due to the small crystallite size, presence of oxygen vacancy surface defects, and decrease in band gap [10].The nanoceria were prepared using the green method followed by the sol-gel method with *Rheum turkestanicum* extract as stabilizing and capping agents. The band gap decreases with the increasing the increased temperature of the annealing [94].The green synthesized CeO_2 NPsusing natural materials like turmeric extract,chestnut,blossom,and pinehoneywith cerium nitrate salt. The prepared samples showed antibacterial,antioxidant, and photocatalytic activity.The band gap energies of the prepared sampleswere 2.8-3.21 eV.The average particle sizeswere1.23,2.61.2.61 and 3.0 nm,and spherical in shape [95]. Another studyshowed that the CeO_2 NPs prepared through the green synthesis route of synthesis using*Dillenia indica*extract showedremarkable antioxidant propertiesthrough the DPPH assay.Therefore, prepared samplesof nanoceriaact as pharmacological agents against various diseases caused by oxidative stress [96].The *C.procera* floweraqueous extractis used for the synthesis of nanoceria of size 21 nm.The prepared sample exhibits 98.64 % of photocatalytic dye degradation of methyl orange.And also showed antibacterial activity against both typesof bacterial strains but higher against the Gram-negative than the Gram-positive bacterial strains [97]. In another method, a polysaccharide biopolymer alginate was used to prepare the nanoceria.The sample crystallite size of 4.6 nmwith spherical uniform size was calculated from the Scherrer equationfrom the XRD pattern [98]. Green synthesis of nanoceria using the orange peel alcoholic extractand cerium nitrate salt.XRD confirmed the cubic nanostructure with the 20-25 nm crystallite size and average diameter of 23 nmby DLS techniques.The synthesized nanoceria have excellent anticancer activity against HeLa cancerous cells.The cell viability in the cancerous cell was lessened to about 92-93 % in different concentrations such as 10, 25, 50, 75, 100, and 125 μg/mlof sample.The anticancer activity was mainly due to the generation of free radicals' species of oxygen like superoxide anion and hydroxyl radical.These species oxidize the macromolecules like DNA,lipids,proteins, and cell necrosis.They also showed the antioxidant properties as the results in the formation of free radical species by using the DPPH method. CeO_2 NPs also showed the photodegradation of MB dye in 30-minute exposure to sunlight.This photocatalytic activity towards the MB was mainly due to the production of holes,hydroxyl, and superoxideradicals [99].In a similar study, the nanoceria was prepared using the*Curcuma longa*(turmeric rhizomes)extract

and cerium nitrate hexahydrate after calcinated at 600 °C for 2 hrs.XRD determined the crystallite size to be 13 nm and FESEM confirmed the spherical shape with the size of nanoparticles around 70 nm. The cell viability of cerium oxide nanoparticles did not affect the BEAS-2B cells with the concentrations of the sample ranging from 5-50µg/well. They were nontoxic to the healthy cells.[100]. The CeO_2 NPs showed a potential heterogeneous photocatalyst that degraded the methylene blue and methyl orange using *Matricaria recutita*extract. The antimicrobial activity (0.15-5 mg of nanoceria) increases with the increase in particle size which is mainly due to the association of reactive free radicals with oxygen species by an increase in the surface area and increased oxygen vacancies [101].

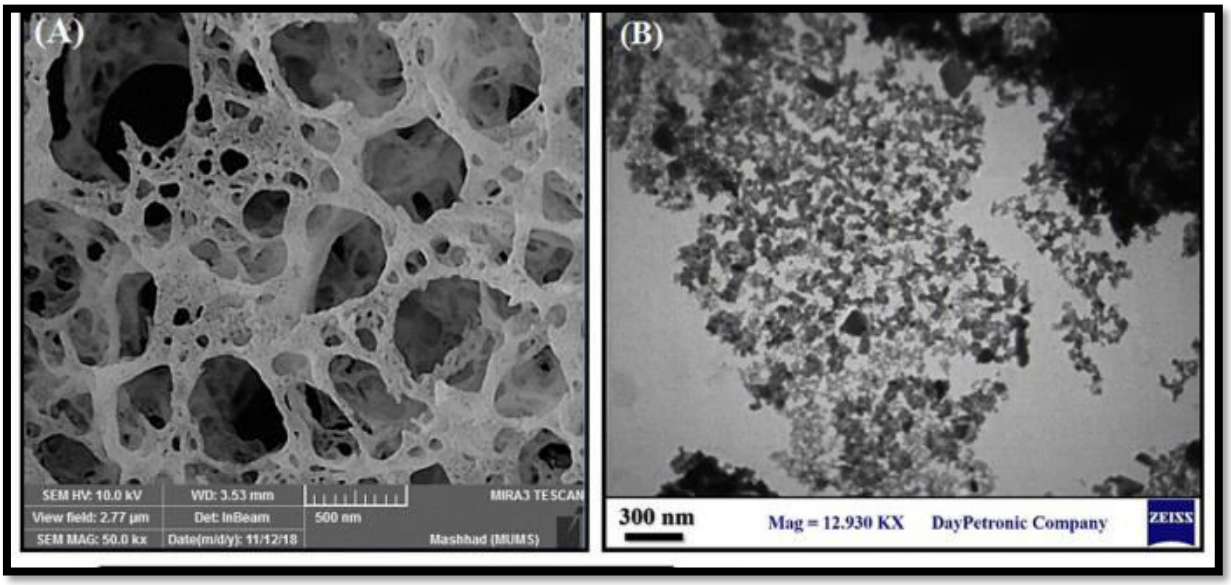

Fig-6-A) FESEM image and**,6-B**)TEM image, asynthesized CeO_2-NPs using extract of *M. sapientum* fruit peel at 400 °C. Reference [102]. Copyright 2018 Springer

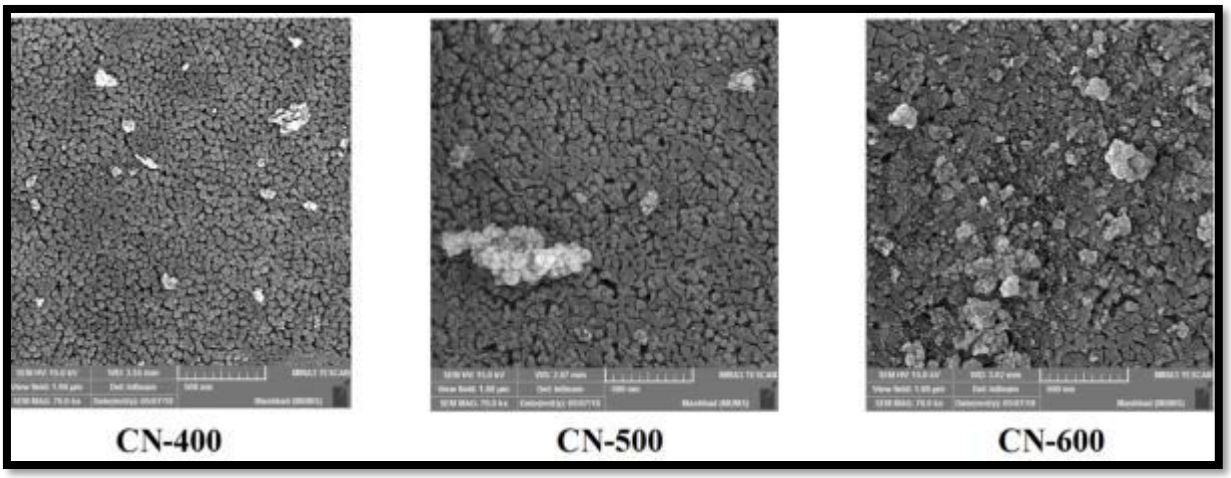

a **b** **c**

Figure- 7a,shows the SEM images of the size of the CN-400 particle is smaller with a more uniform morphology,**Fig.7b)** and c) showed the SEM images of CN-500 and CN-600 increasing the calcination temperature resulted in the particle

agglomeration.via green synthesis by using *Cydonia oblonga miller* (Com) seeds extract Ref[103].Copyright 2014 Elsevier

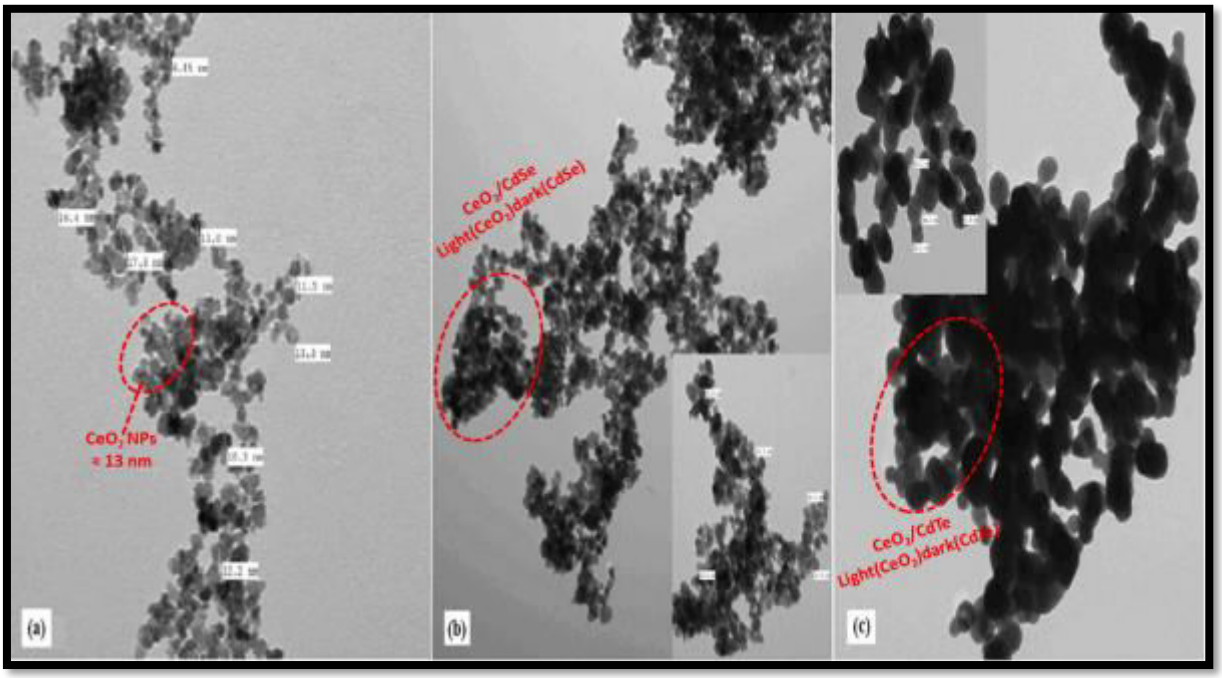

Fig.8-TEM images of (a) bare-CeO_2 NPs (b) CeO_2/CdSe nanocomposite (c) CeO_2/CdTe nanocomposite Reference [104]. Copyright 2021 Elsevier

3.Applications: Cerium oxide nanomaterials are very importantin diverse fieldslike biological,catalyst, and various other fields. The various properties are mainly derived from the ability of the nanoceria to possess two oxidation state and their conversion fromthe Ce+4 state to the Ce+3 state. And the presence of oxygen defects in the lattice structure [105].

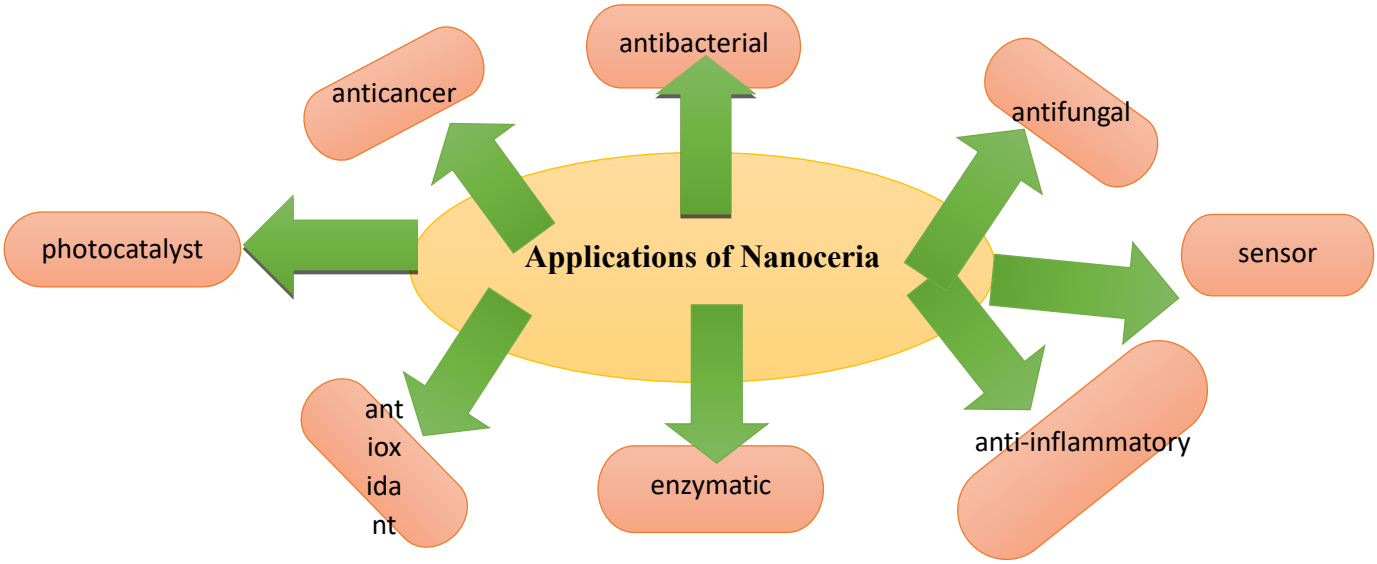

3.1. Photocatalytic Activity: The photocatalytic activity was a series of reactions carried out by the photocatalyst and remained unchanged at the end of the process. In the photocatalytic reaction, the catalyst has a small energy band gap. The photocatalytic process occurs in the absorbed phase. Semiconductors were mainly the oxides and sulfides of metals irradiated with photons, whose energy is equal to or higher than the band gap energy. The absorbed photon created the electron-hole pair, which dissociated into free photoelectrons in the conduction band and photo-holes in the valence band. The OH•, and O_2• highly reactive free radicals were generated by these holes and free electrons by the water and O_2 species respectively. These reactive oxygen species then degraded the dye molecules into smaller molecules which are non-hazardous forms The possible mechanism was proposed for the photocatalytic degradation process as:[106].

$$CeO_2 + h\nu \rightarrow e^-_{CB} + h^+_{VB}$$
$$e^-_{CB} + O_2 \rightarrow O_2^{\cdot-}$$
$$O_2^{\cdot-} + MB \rightarrow Product$$
$$h^+_{VB} + H_2O \rightarrow HO^{\cdot} + H^+_{aq}$$
$$HO^{\cdot} + MB \rightarrow Product$$

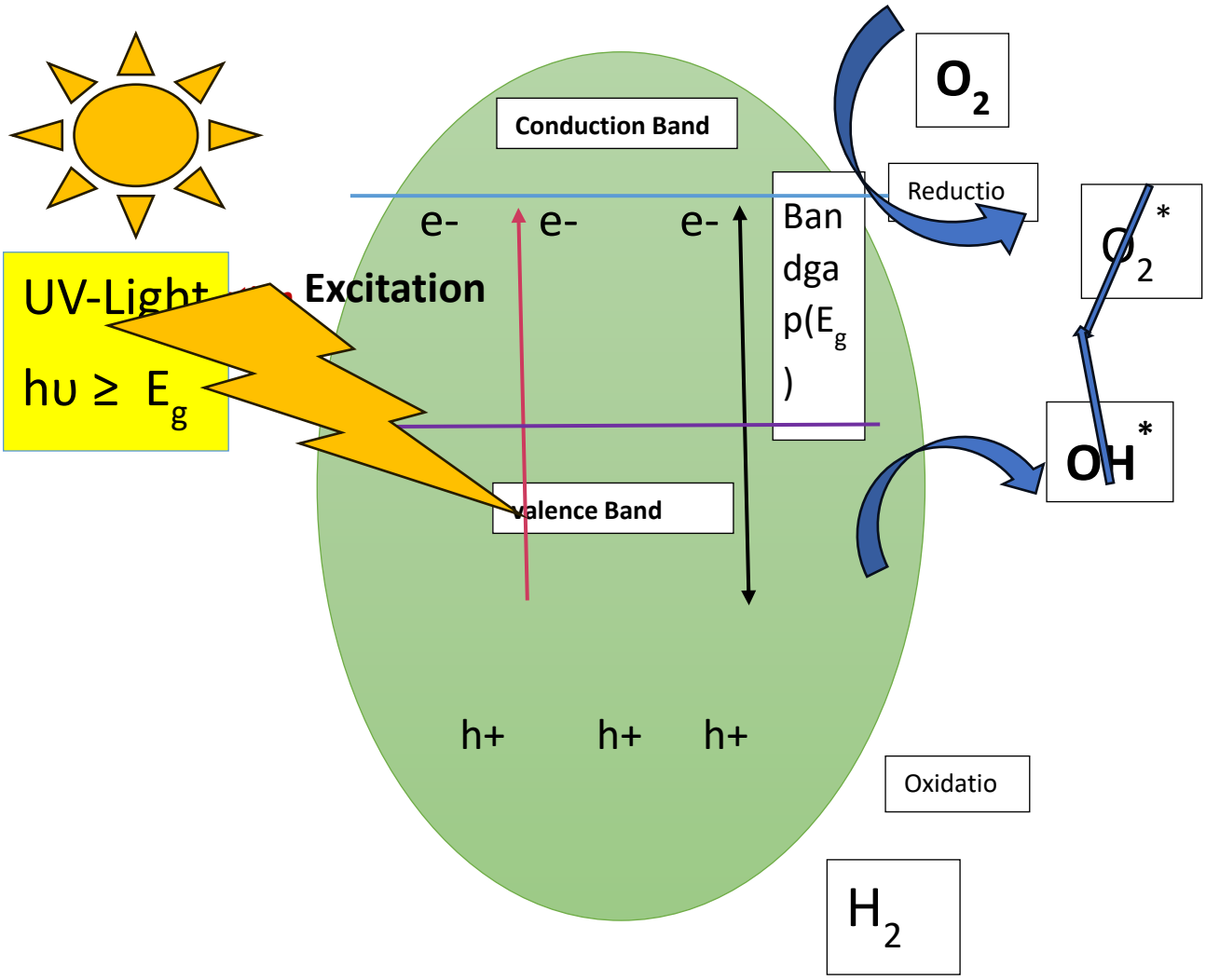

Fig.9-Diagrammatic Presentation of the Photocatalytic Activity of nanoceria against thedye degradation by the free radical species.Reproduction of Ref.[106]. Copyright2022 Elsevier.

The various other parameters including crystallite size, morphology, phase composition, surface area, and structure also affect the phenomenon.

The surface of the CeO_2 QD of 1-10 nm size is affected by the fabrication in the structure of nanomaterials by surfactants-assisted cerium oxide NPs.The surfactants decreasethe size of the nanomaterials about to the range of QD that is. 1-10 nm.The prepared QDacted as a catalystfor degrading MB at about 99.16 % under sunlight.The easy conversion of soluble Ce+4 to Ce+3that easily oxidized the Fenton reagents to produce $OH^{\cdot}$ Which is a more reactive species than the peroxide to react with the MB species [107]. In another study biosynthesized CeO_2-NPs of size (21 nm) were prepared using *C. procera* flower,and showed photocatalytic activity against MO to degradedMO dye about 98.64 % of 50 minunder the sunlight (457 nm -λ) [108].Similarly, thespherical-shapednanoceria of size (4-13 nm) prepared by usingbanana peel showed 81.7 % photodegradation of AO7 dye in 120 min under visible light [102].

The presence of free radicals and thesurface area of the nanostructured hasa great impact on the catalytic activity.Recently nanoceria was prepared through the green method using *Cydonia oblonga miller* seeds. The photocatalytic degradation of Rhodamine B dye under UV-A light was approximately 94 %. The excellent photocatalytic capacity of prepared materials is because of the high surface oxygen vacancies. The surface vacant oxygen sites can take the conducting electron and decrease the recombination of electron-hole pairs. The hole reacts fast with dye molecules and degradesthem [103].Sachin Kumar et alproposed the following reaction steps for photocatalytic degradation [48].

$CeO_2 + h\nu \rightarrow CeO_2 (h^+ + e^-)$

$CeO_2 (h^+) + H_2O \rightarrow CeO_2 + OH^{\bullet} + H^+$

$CeO_2 (h^+) + OH^- \rightarrow CeO_2 + OH^{\bullet}$

$CeO_2(e^-) + rGO \rightarrow CeO_2 + rGO (e^-)$

$rGO (e^-) + O_2 \rightarrow rGO + O_2^{\cdot -}$

$OH^{\bullet} + \text{MB dye} \rightarrow CO_2 + H_2O + SO_4^{2-}$

$O_2^{\cdot -} + \text{MB dye} \rightarrow CO_2 + H_2O + SO_4^{2-}$

A nanocomposite of magnetic multi-walled carbon nanotubescerium dioxide is created hydrothermally.CeO_2 photocatalytic properties have been enhanced for methylene blue (MB) degradation (97.5%). The MMWCNTs-CeO_2 system is employed in the treatment of organic contaminants in wastewater[109].Graphene oxide coated(5 wt %)-CeO_2 nanocompositehasa great influence on MB degradation under visible radiation. Graphene-oxidenot only decreases the nanoceria particlesize but also enhances the separation ofthe photogenerated electron-hole pair.The possible mechanismis that in irradiation under visible lightthe electronis transferred from the valency band to the conduction band.The

electron on the conduction band of CeO2 easily migrated to the surface of the GO in the nanocomposite.The electron accumulated on the GO surface interacts with the O_2molecules to produce the $O_2^{-\cdot}$, whichcauses the partial decomposition of MB.The hole in the VB is directly involved in MB degradationand decreases the recombination rate of the electron-hole pair to enhance the photocatalyticactivity of the catalyst [110].

Green method usingD(+)-glucosethe cerium oxide–carbon microspheres were developedusingthe hydrothermal method. Thehybrid microspheres were 5 μm in size and were an excellentcatalyst in salicylic acid degradation using ozone[40]. The Pd-doping on CeO_2showed the potential generation of the new energy level in the band structure of CeO_2. Thedecreasing band gap from 3.0 eV to 2.8 eV by the presence of Pd^{+2}.The trappingof electrons by the sub-band states ofPd^{+2}/Pd^{+3} andPd^{+}/Pd^{+2}.The properties of the trapping decrease the electron-hole recombination process resulting in improving the Pd-dopedCeO_2 photocatalyst performance.And increased5timesmethyl orange dye degradationthan CeO_2photocatalyst [89]. A similar study of Ag/CeO_2 nanostructured using tartaric acid as a fuel in a simple solution combustion reaction. The synthesized Ag–CeO_2 materials were porous in nature of ~5–7 nm average pore size.The prepared products were an excellent photocatalyst to degrade 100% Rh B dye in 150 min[111]. V_2O_5-CeO_2 nanocompositeshowed a remarkable photodegradation of MB dye above 98 % in just 25 min.The V_2O_5-CeO_2, in the presence ofscavenger agent H_2O_2, photodegrades the MB [112].

The morphology and the BET also affect the catalytic activity.The nanoparticles of CeO_2 were prepared using CTAB (surfactant) by co-precipitation process.The nanorods and spherical nanoparticles are developed withan average crystalline size of 5.0-4.4 nm.The proposed mechanism for the catalytic degradation of Congo Red dyeis given below [113]:

$Ce^{3+} + O_2 \rightarrow Ce^{4+} + O_2^-$

$Ce^{4+} + H_2O \rightarrow Ce^{3+} + \cdot OH + H^+$

$O_2^- + H^+ \rightarrow HO_2$

$2HO_2 \rightarrow H_2O_2 + O_2$

$H_2O_2 \rightarrow 2\cdot OH$

$CR + \cdot OH \rightarrow CR_{ox}$(intermediates) $\rightarrow CO_2 + H_2O$

Another study has shown that cerium oxide nanoparticles are irregularly shaped and showed some agglomeration to form large-size particles(0.5-2.0 μm) due to the rapid increase in the temperature.TEM images confirmed the almost spherical with an average diameter of 15 nm which is higher than the XRD (12.2 nm). The band gap and surface area are 2.85 eV and 47.7 m^2g^{-1}. The cubic phase CeO_2 has the presence of +3/+4 in the sample. Due tothe cubic phase and the presence of +3/+4 in the samplewitha high band gap of about 2.85 eV, photosensitized by the light absorption to form a (e^- /h^+) pair.That generation of electrons in the conduction and hole in the valency band both leads to the formation of reactive species of oxygen and hydroxyl radicals leading to the formation of degrading

dye molecules[114].Alia Raees et al 2021 in theirstudy used co-precipitation to create a nanocomposite of CeO_2/CuO. The average particle size was between 20-30 nm. Under visible light, they demonstrated excellent photocatalytic activity for methylene blue. The mechanism of methylene blue degradation is dependent on electron-hole separation. The visible light radiation energy was determined by the band gap between the valency band and the conduction band, which resulted in the excitation of valency electrons from the valency band to the conduction band, which created a hole in the VB and energized electrons in the CB. The production of free radicals serves asa platform for dye degradation.The synthesized nanomaterials demonstrated a very fast and efficient dye degradation catalyst towards methylene blue(MB), with times of 150 minutes and 85.66%, respectively. Due to particle aggregation on a heterogeneous surface, particles of size 25-30 nm were formed from SEM data[115].Arthira Krishnan etal (2021) modifiedthe catalytic properties of the nanocomposite CeO_2-$Fe_2O_3$by Sndoping.The electronegativity and the ionic radii of the Ce^{+4}weresimilar to that of Sn^{+4}, during theformation of the nanocompositethe Ce ions were replaced by the Sn. That affects the size of the nanocomposite from 20 nm to 12 nm. No regular surface morphology of the nanocomposite was observed. The compositeaverage grain size is 40 nm. This study showed that the concentration of the dopant ion affects the efficiency of the photodegradation of the catalyst[116].CeO_2-Y_2O_3nanocompositephotodegrades the rhodamine-B 98 % using catalyst/H_2O_2 at 9 pHalmost at 150 min.The synergic effects between CeO_2-Y_2O_3have an importantrole in enhancing the photocatalytic activity of the catalyst.The possible following steps inthe mechanism of nanocatalystare given below:[117]

$CeO_2 + h\nu \rightarrow CeO_2\ (e^- + h^+)$

$Y_2O_3 + h\nu \rightarrow Y_2O_3(e^- + h^+)$

$Y_2O_3 + CeO_2 \rightarrow CeO_2\ (e^-)$

$e^-\ (_{CB}\ CeO_2) + O_2 \rightarrow O_2^{-\cdot}$

$O_2^{-\cdot} + H_2O \rightarrow OH\cdot$

$h^+(_{VB}\ Y_2O_3) + H_2O \rightarrow Y_2O_3 + H^+ + OH\cdot$

$RhB + O_2^{-\cdot} + h^+ + OH\cdot + ROS \rightarrow$ degradation products

N.Sabari Arul 2012study showed that the Co-dopednanoceria wereprepared using the co-precipitation method withoutsurfactants.The sample was characterized using XRD confirming thedecrease in the lattice parameter due toCo doping.The morphology of the sample suggested by FESEM, and HRTEMimages showed the aggregation of the nanoparticles to form the nanorods of 100-300nmlength and 10 nm diameter.The surface morphology confirmed the porous structure.The BET

surface area increases by about 131 m^2/g more than the undopedsamples. The resultsshowed 100 %photodegradation of AO7 with 10 h exposure[118]. In another study Co-doped nanoceria prepared by co-precipitation method using ethanol as solvent,homogenous size distribution of 5-12 nm nanoparticles were formed.The doping of Co increases the oxygen defects and the band gapin the CeO_2NPs.The photocatalytic degradation efficiency of MB increasesupto 98.7 % [119].The surface defects at the catalyst surface also have important factors that affect the photodegradation efficiency.The photocatalytic degradation of organic dyemethylene blue (MB) under dark,sunlight, and UV radiation.In dark the dye degradation efficiency was much lesser than in the other two conditions.The cubical nanoceria showed a70 % efficiency than the spherical-shaped nanoceria which have about 50 %.The C-CeO_2has better degradation capacity over the S-CeO_2 due tothe high content of surface defects that enableto capture of electron-hole-pair easilyand less amount of energy required as the small band gap of about 2.82eV in C-CeO_2than the S-CeO_2 that induced the photocatalytic reactions.It also observed that the concentration of the nanoparticles affected the degradation efficiency of S-CeO_2.The increase in the concentration above 1.0 gL^{-1}(maximum degradation rateis 72 %), whichcauses the agglomeration in theS-CeO_2 particles to form clusters hence the decrease in the charge separation than the recombination ratio,shows the lowerefficiency of the nanoparticles.The concentration of the dyes also affects the efficiency of dye degradation from 83.5% to 54 % when concentrationwas increased from10 to 30 mgL^{-1}respectively[76].The OPL-mediated nanoceria of spherical shape, crystal size 5.2 nm can remove 92.24 % phenol in 360 min under visible radiation[120].The deep eutecticsolvent-mediated synthesis of nanoceria was an excellent method to enhance the photocatalytic efficiency of the degradation of flumequine,effluents from the pharmaceutical industries.The DES-ceria have a much higher surface area(130.2 m2/g), which provided the high accumulation of the FLU molecules on the active site of the catalyst[121].The irregulararchitectureshape with a clear boundary and micro/meso surface particles of X-CeO_2exhibit excellent properties of photodegradation of MB under UV-visible radiationup to six cycles. The photocatalyst hashigh stabilityin the generation of charge separation between CB and VB. TheO_2^{-}·and OH·generated from oxides and $OH^{\cdot}$ radicals from OH^{-} ion in CB and VB respectively [122].Thepresence of plenty of oxygen vacancyis also responsible for the photocatalytic degradation of dye.Theseoxygen vacancies in the nanoceria latticewhich is the main source of adsorption of water molecules,act as the active sites for the water dissociation. The doping of Sm and Gd increases thelattice-free electrons and holes in nano CeO_2preparedthrough the microwave method.The doping affects the shape,size, and morphology of the nanoceria which directly affects the photocatalytic activity of the catalyst. Sm and Gd doped nanoceria 100 % photodegrade the MB in 16 and14 hrs respectively into safe and nontoxic products[123]. The size and the surface area of the nanoparticlesplay an important role inthe photodegradationactivity[124].CeO_2/CdSe nanocomposite

showed photocatalytic activity(100 %)against Congo red dye for the wastewater treatment[104].The CeO_2/rGOshowed excellent catalytic properties due to the 2Dπ -conjugation system of rGO that eased to generate the electron hole and movement of electrons from the valence band to conductionand decreaserecombination witha hole that enhances the photocatalytic activity[125].

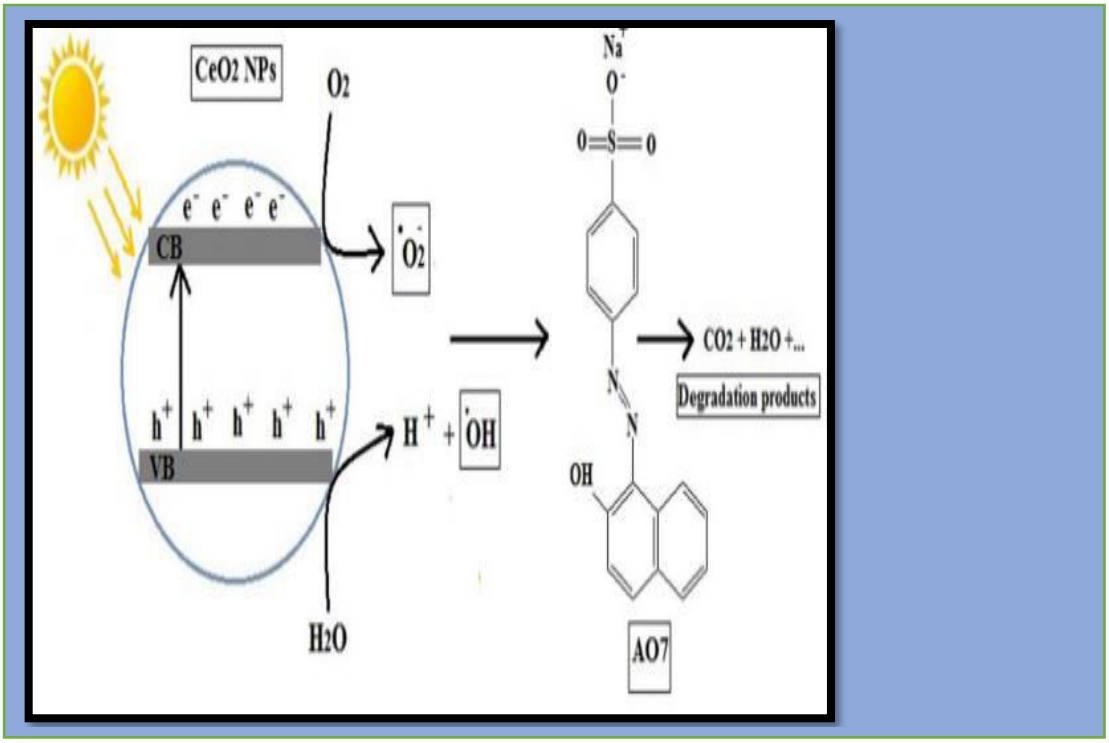

(**A)**

(A)

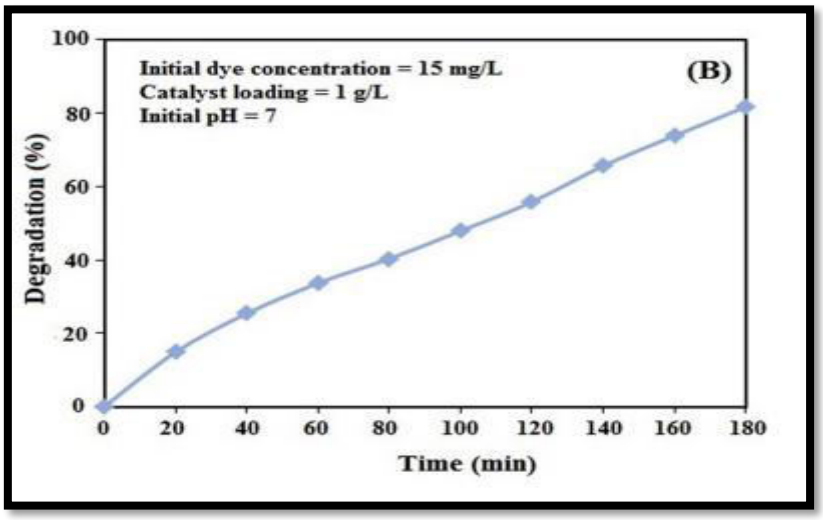

Fig.10-(A) Suggestion mechanism of photocatalytic activity of synthesized nanoparticles in degradation of Acid Orange 7 dye.(B) Photocatalytic degradation of AO7 under synthesized CeO_2-NPs at 400 °Cusing biosynthesized*Musa sapientum* peel extractRef[102]. Copyright 2021 Springer

Table 1– Differentmethods of synthesisofnanoceria using chemical and green and their Photocatalytic activity, dose of catalyst, Volume/conc. of dye solution, and removal efficiency

S. No.	Photocatalyst	Method	Size by SEM &TEM/Morphology	Pollutant	Dose of catalyst	Volume/conc. of dye solution	Removal efficiency	Time of illumination	Ref.
1	CeO_2	Controlled synthesis by hydrothermal	Cubical	Methylene Blue	1.0 g/L	10 mg/ L	C-CeO_2-83.5 % S-CeO_2-60 %	210 min	[76]
2	CeO_2	Co-ppt (CTAB)	15.39 nm	Methylene Blue	0.1-0.7 g/L	10 mg /L	76 %	240 min	[86]
3	Pd - CeO_2	Homogenous precipitation	10-20 nm /spherical with high agglomeration	methyl orange	0.2 g/L	20 mg/L	92 %	120 min	[89]
4	CeO_2	leaves of *Rheum turkestanicum*	30 nm/spherical agglomerated and uniformed	rhodamine-B methyl orange MB	120 mg/ L	1×10^{-5} M	82 % 71 % 33 %	180 min	[94]
5	CeO_2-NPs	Biosynthesis from *Matricaria recutita*	12 nm	Methylene Blue &and methyl orange	1 g/L	60 mg/L	93.0 %	108 min	[101]
6	CeO_2	Green synthesis	4-13 nm	acid orange 7	15 mg/ L	1.0 g/ L.	81.7 %	180 min	[102]

		by banana peel							
7	CeO_2/CdSe and CeO_2/CdTe	hydrothermal	20.7/20 nm	Cong Red	1 g/L	5×10^{-5} M	100 %	150 min	[104]
8	CeO_2	Sonochemical method	35-38 nm spherical with porous nature	Methylene Blue	2.4 g/L	20 mg/L	90.4 %	90 min	[106]
9	CeO_2	Green synthesis using *Calotropis procera* leaf extract	21 nm	methyl orange	1.0 g/L	$1x10^{-5}$ M	98 .64 %	50 min	[108]
10	MMWCNTs - CeO_2	Hydrothermal	-	Methylene blue	1 g/L	$5x10^{-5}$ M	97.5 %	120 min	[109]
11	CeO_2-graphene oxide composite	Alcohol-thermal method	-	Methylene Blue	0.1 g /L	20.0 mg /L	81 %	240 min	[110]
12	Ag- CeO_2	Solution combustion method	Nanoflakes with porous nature.	Rhodamine B	1.5 g/L	2.08 x 10^{-5} M	100 %	150 min	[111]
13	V_2O_5- CeO_2 Nanocomposite	Precipitation-thermal decomposition	-	Methylene Blue	0.2 g/L	10 mg /L	Above 98 %		[112]
14	CeO_2	green chemical precipitation method (cationic surfactant CTAB)	4.3-5.0 nm Spherical nanoparticles and nanorods	Azo dye Congo red	10 - 250 mg/L	10-100 mg/L	Nanoparticle-90 % nanorods - 97%,	360 min	[113]

15	CeO_2	Microwave mediated hydrothermal	15 nm/single cubic phase spherical	Alizerinred S Eriochrome black -T	0.8,2.0, 6.7 g/L 0.6,2.0, 6.8 g/L	100 mg/L 100 mg/L	100 % 100 %	120 min	[114]
16	CeO_2/CuO Nanocomposite	Co - ppt	20-30 nm	Methylene Blue	1 g/L	10 mg/L	85.66 %	150 min	[115]
17	Sn doped (5 %)-CeO_2 - Fe_2O_3 composite	Thermal decomposition	15 nm	Methyl Orange and Methylene Blue	1.0 g/L for both	10mg/L for both	94.65 % MB & 100 % MO	120 min	[116]
18	CeO_2/Y_2O_3 nanocomposite	Hydrothermal method (NaOH)	10 nm/ nanopowder	Rhodamine B dye	5g/L	20 mg/L	98 %	150 min	[117]
19	Co-doped CeO_2	Co-precipitation (NH4OH)	nanorods	Azodyes acid orange 7	4 g/L	0.2 M	100 %	240 min	[118]
20	Co- CeO_2 (doping 6 % of Co)	co-precipitation	5-12nm	Methylene Blue	1 gm/L	15 mg/L	98 %	420 min	[119]
21	CeO_2-NPs	*Elaeis guineensis* leaves	13-16 nm/ uniformly agglomerated	phenol	1.0 g/L	50mg/L	92.24 %	360 min	[120]
22	CeO_2	PVP - assisted hydrothermal	Length 20 µm-width 4 µm/ Micro or /mesopore	Methylene Blue	1 g/L	40 mg/L	99.9 %	120	[122]
23	Sm & Gd doped CeO_2	Microwave	15-29 nm/nanorods	Methylene Blue	1g/L	1.7×10^{-6} M	99.6 %	9 hrs	[123]
24	CeO_2	Solution combustion using (EDTA)	35 nm/spherical nanoparticl	Trypan blue	0.4 gm/L	5-25 mg /L	100 %	135 min	[124]

			es						
25	CeO_2/rGO	hydrothermal	6.23 nm	Direct green	15g/L	20 mg/L	80 % UV	120 min	[125]
26	CeO_2	*Elaeis guineensis* leaves	13-16 nm/ uniformly agglomerated particles	phenol	1.0 g/L	50 mg/L.	92.24%	360 min	[126]
27	CeO_2	Marine oyster	15 nm	Methylene Blue	150 mg/L	150 mg/L	99 %	60 min	[127]
28	CeO_2	Green synthesis *Moringa oleifera*	45 nm spherical	Crystal violet	5 mg/L	10 mg/L	97.5 %	60 min	[128]
29	CeO_2	Green *Jatropha curcus*	18-25 nm	acetaldehyde	-		99.6 %	-	[129]
30	CeO_2	Green synthesis *A. indica* leaf extracts	10-15 nm with a uniform size	Rhodamine B	10g/L	10 mg/L	96 %	120 min	[130]
31	Eu doped CeO_2	Glycine assist hydrothermal	15-20 nm, spherical with some agglomeration	Cong Red			67 % UV–visible	120 min	[131]
32	Er- CeO_2	Hydrothermal method	20 nm and diameter35 nm/nanorod	Rhodamine B dye	5 g/L	20 mg/L	94 %	40	[132]
33	CeO_2	hydrothermal	23 nm spherical/	Methylene Blue	0.5 g/L	1mmol	-	-	[133]
34	CeO_2	Precipitation	Nanorods, 82.3 nm	methyl orange	5g/L	$1.5 x10^{-4}$ M	50 % UV	80 min	[134]
35	CeO_2	Solution combustion using watermel	Agglomeration with irregular morpholog	Methylene blue	10 mg/L	10 mg/L	98 %	180 min	[135]

		on juice	y						

3.2. Biological Activity: The cerium oxide nanoparticles showed potential applications in the biological fields. They showed anticancer, antioxidant, anti-inflammatory, and antimicrobial activity. The biological properties of nanoceria are mainly due to the existenceof two oxidant states, Ce+3 and Ce+4.The interchanging of these two states can form an oxygen vacancy on the surface of the nanoceria. The band gap energy of the nanoceria is responsible for creating holes and the reactive free radical species. Both these factors are responsible for the biological activity in nanoceria.

3.2.1. Antibacterial activity

The antibacterial activity of the nanomaterials was counted regardingthe various parameters.These parameterslike size, surface morphology, surface area,the charge on particles, and the reaction medium.Theantibacterial mechanism occurs mainly two-stepprocess. In step first, the nanomaterials are adsorbed on the surface of the bacterial membrane. Since the bacterial membrane is negatively charged on the surface, that causes the interaction between the cell wall and the nanomaterials.The second step after the adsorbed onto the bacterial membrane causes oxidative stress and interferes with the internal nutrients of the cell[136].

Green synthesis of cerium oxide nanoparticles using *Prosopis juliflora* leaf extract ultrasound-assisted method evaluated the antibacterial activity against both Gram-positive (G+) bacteria and Gram-negative (G-) bacteria.The disc diffusion assay was performed by a zone of inhibition test witharound CONPs MICs, about 0.1 ml. In *P. aeruginosa, P. vulgaris*, showed mild to moderate activity while the case of*S. aureus* and *S. pneumonia* showed the highest antibacterial activitydue to their different cell membrane andcellwall composition[36]. Ag/CeO_2composite(12-31 nm)has an average porous nature (5-7 nm).They exhibitexcellent antibacterial activity against both gram-positive and gram-negative bacterial strains.The minimum inhibition concentrationof the Ag/CeO_2samplewasobserved at 3.125 μg/ml and 6.25 μg/ml.The possible antibacterial mechanism for cell death by nanostructures is due to the production of ROS on the surface of the cell wall, which damages the bacteria's cell wall, causing cytoplasm leakage and ultimatelycell death[111].The antibacterial activity was tested using a disc diffusion test against theGram-positive organisms and Gram-negativeorganisms. Theantimicrobial activitywas 100% against Gram-negative organismsthan the others[73].Abbas et al2016 prepared citric acid-basednanostructures of ceria by giving hydrothermal and agingtreatment. The crystalline size of 9 nm was calculated by XRD. The SEM images revealed multilayer nanosheets to form microspheres. The average size was about 40 nmas compared to nano spherical particles were 30 nm in size.The agar disc diffusion test demonstrated that the nanosheets have higher antibacterial activity than the nanospheres. The presence of oxygen vacancy over the surface enhances the interaction with the cell wall and generates the ROS that causes ultimately cell death [75].LU Xiao-wang et al

2012prepared Ag/CeO_2mesoporous with pore size in samples 5-7 nm.The doping concentration affects the pore size and BET surface areas. The 5% Ag/CeO_2 mesopores observed the complete retardation of bacterial growth by usingthe agar dish method against gram-negative bacterial strain.The bacterial activity was mainly due to the Ag ion on the mesopores of the sample that was producedcombined with the cell membrane.The accumulation of ions on the surface of bacteria thatrupture the cell membrane and intracellular fluid leakage brings cell death [137].In the recent study shape-controlled synthesis of CeO_2 NPs showed antibacterial activity of C-CeO_2 and S-CeO_2 was examined against different bacterial strains using the disc-diffusion method with the standard drug oxytetracycline.The C-CeO_2NPs effectively act on all bacterial strains as compared to theS-CeO_2due to their cubical shape, surface-to-volume ratios, and exposed crystal facets that presenta high amount of oxygen vacancies[76].The surfactants-based(SDS, CTAB,PVP)ceria nanoparticles were synthesized using the hydroxide mediate method.The different surfactantsaffectthe surface and morphologyof the developed nanomaterials.The grain size was found to beinthe 37.5-43.5 nm range withspherical-shaped morphology of the nanoparticles.The antibacterial activity was observed at100% in gram-negative bacterial strains*Proteus vulgaris*than in the gram-positive strains*Corynebacterium diphtheria*and*Sarcina lutea*.The size and shapeof nanomaterials influence the antibacterial action as the interaction with the cell wall of the bacteria or as the concentration increases leadsto the internalization of the nanoparticles and causes the toxicity of the bacterial cell[138].The dopant nanoceria inhibits bacterial growth due to their smaller size and large surface area.The cell walls of both the gram-positive and gram-negative bacteria are negatively charged.The interaction between the cell wall and the positively charged nanoparticles changes the action of the electron transport chain in bacteria. Recent studies proved that ROS generation is deeply associated with the dopant that modified the structure of nanoparticles.Green facile synthesis of Ag-doped ceria nanoparticles using saliva seeds enhanced the antibacterial activity against both bacterial strains[139]. Thesamarium (Sm) doped cerium oxide (size 43-58 nm)had excellent antibacterial activity due to the Sm^{+3} doped metal as the presence of reactive oxygen species produced the oxidative stress that causes bacterial cell death [140]. Another study reported that Gd-doped CeO_2 nanoparticles of size 57.4-58.3 nmin cube and square shape showed excellent antibacterial activity. The main reason was the smaller-sizedparticles easily entered into the cell wall which causes bacterial cell death [81].The green synthesized nanoceria by using *Acalypha indica* leaf has been reported the inhibit bacterial activity by more than 90 %.The mechanism for the antibacterial activity was that the cellular proteins became inactive as the nanoceria generated the hydrogen peroxide that causes cell death [141]. Engineered cerium oxide nanoparticles were produced through the hydrothermal method with modified surfactants and templates free showed antibacterial activity [142].The Co-doped nanoceria was prepared by the

hydrothermal method.The face-centeredcubic with crystallite of 17-20 nm in size.The doping concentration of Co decreases the size of crystallitewhichaffects the antibacterial activity.The doping concentration was increased the antibacterial activity increasedagainst the four pathogenic bacteria.The antibacterial mechanismmay be due to the interaction between the bacterial cell wall and the nanoparticles.The smaller the size higher the interaction between them and the nanoparticles penetrate the cell andROS is generated that causes cell death [143]. Transitionmetal ions doped nanoceria prepared through the green method showed excellent antibacterial activityas compared to the pure CeO_2 in both bacterial strains.The possible mechanism through which it acts on the microbial is by the direct interaction with the microbial cells or to produce the secondary products that cause cell death [92].Mohammad Altaf et alreported thegreen synthesized nanoceria from *Acorus calamus* extractsantibiofilm activity againstboth gram-positive and gram-negative bacterial strains.The prepared nanoparticles successfully inhibition of biofilm of *E. coli, P. aeruginosa*, and *S. aureus*in all concentrations.The possible mechanism wasthe inhibition of exopolysaccharides (EPS)by theCeO_2-NPswhich is responsible for the biofilm production in the bacteria and the production of ROS[144].Biosynthesizedcerium oxide NPs from *Coriandrum sativum* leaf extract showedexcellent antibacterial activity against*P. aeruginosa*and*K. pneumonia*(gram-negative strain).as compared to *Bacillus cereus,Bacillus subtilis* (gram-positive) [145].

Table 2– For the Antibacterial activity of nanoceria using chemical and green methods of synthesis, the size of nanoparticles, morphology,and concentration of nanoceria dose.

S. No.	NPs	Dopant	Size in nm	Morphology	Method	Concentration of dose	Types of Bacterial strain	Zone of inhibition (mm)	Ref.
1	CeO_2	-	-	Spherical	Green synthesis*Leucas aspera* (LA) leaf extract	50-100 µg/L	*E. coli* *S. aureus*	4.67 3.33	[10]
2	CeO_2	Gd	58.3-57.4^D	Cubic and square shape of uniform size	Hydrothermal	1 mg/ml	*E. coli* *B. cereus* *S. aureus* *S. typhi*	28 26 23 26	[81]

3	CeO_2 NPs	Transition metal ion doped	9-16 ^{D}	Cubic-spherical	green synthesis	-	*K. pneumonia* *S. aureus* *S. dysenteriae* *E. coli* *P. aeruginosa* *S. pneumonia* *P. vulgaris*	Active Active Active Active Active Active Active	[92]
4	CeO_2	-	14.95^{D} 5-20^{T}	Cubic and spherical	*Aspergillus niger*	10 mg/mL	*Streptococcus pneumonia* *Bacillus subtilis* *Proteus vulgaris* *Escherichia coli*	10.67 10.33 8.33 6.33	[93]
5	CeO_2	-	35^{D} 42^{T}	cubic	Solution combustion	500-1000 µg/L	*P. aeruginosa* *S .aureus*	4.5 Not seen	[124]
6	CeO_2	-	45^{D}	aggregate spherical	Microwave-assisted using M. oleifera peel	25 µL	*E. coli* *S. aureus*	7 5	[128]
7	CeO_2	Eu	15-20^{D}	Spherical with agglomeration	*Glycine assisted Hydrothermal*	-	E. coli S. aureus	4.2 2.2	[131]
8	CeO_2		36 ^{D}	Agglomeration with an irregular porous	Solution combustion using watermelon	1000-500 µg/L	*Klebsiella aerogenes* *S. aureus*	1.00 1.67	[135]
9	CeO_2	-	40-100 ^{S}	cubical shape	Hydroxide mediate method	20 µl 100 % conc.	*Proteus vulgaris* *Escherichia coli* *Corynebacterium diptheriae* *Sarcina lutea*	5 3 Not seen Not seen	[138]

10	CeO_2	Ag	62^D	Uniform spherical	*Salvia* seeds	15 μL	S. aureus P. aeruginosa	_ _	[139]
11	CeO_2	Sm	58.3-43.47^D	Octahedral	Hydrothermal	1 mg/ml	*E. coli* *B. cereus* *S. aureus* *S. typhi*	20 22 25 24	[140]
12	CeO_2	Co	17-20 ^{D}	small leaves or feathers like on cubic shape	hydrothermal	1mg/ml	*E.coli* *S. aureus* *B. cereus* *S. Typhi*	24 23 27 25	[143]
13	CeO_2	-	2 2.03 ^{D} 16.92^T	Spherical and pseudo-spherical	Green synthesis using *Acorus calamus*extract	1,600 μg /ml	S. aureus P. aeruginosa E.coli	Active Active Active	[144]
14	CeO_2/CdO	nanocomposite	27^D 15 –40^S 25 to 5^T	spherical in shape, heterogeneous with more cavities	Precipitation and hydrothermal method	200 μg/ml	*S. aureus* *S. pyogenes* *P. aeruginosa* *K. pneumoniae*	P H 12 14 20 16 30 35 8 13	[146]
15	CeO_2	-	5 ^{T}	Spherical with some aggregation	Neem and ginger extract	100 mg	S. mutans S. aureus C. albicans Enterococcus faecalis	11 19 9 9	[147]
16	CeO_2	-	30 ^{D} 36^T	Porous surface homogenous	Green synthesis using Abelmoschus esculentus	30 μg/ml	S. aureus K. pneumonia	21 19	[148]
17	CeO_2	Fe	22 ^{D} 27 ^{PSD}	Nearly spherical with some irregularly shaped aggregates	Co-ppt using Xanthan gum	128 μg/ml	*Pseudomonas aeruginosa, Listeria monocytogenes*	active active	[149]
18	CeO_2	-	13.56^D	Nanoparticles with	*Coriandrum sativum* leaf	50 μl	*P. aeruginosa* *K.*	12 9	[145

				slight agglomeration	extract		*pneumonia Bacillus cereus, Bacillus subtilis*	56	]

D- XRD, T-TEM, S-SEM

3.2.2. Cytotoxicity: The cytotoxicity of the cells was determined by the cell viability test in different assayed methods.The cytotoxicity of the cells has been determined by different parameters. TheROS(reactive oxygen species) generally causes oxidative stress in the cell as the damage to protein, DNA, and cell membrane.The mitochondrial activity also expresses cell viability.The cerium nanomaterials showed cytotoxicity in the cell viability test.The nanoparticles of cerium oxidewere synthesizedthrough the supercritical methodtodevelop nanoparticles ofdifferent sizes. The cytotoxicity was assessed by using the MTT test using BEAS-2Bcell lines of human lung epithelial cells.The cellswere exposed tonanoparticles (5,10,20,30,40 μm/ml) of 30 nm sizecausing cell death.Theincreased ROSlevel caused adecrease in GSH.The genesthat are responsible for oxidative stress were induced(40 μm/mlof 30 nm particles) including catalase, glutathione S-transferase, heme oxygenase-1, and thioredoxin reductase at exposure time 4 h.Howeverhousekeepinggeneslike actinare not changed by nanoparticles.The chromatin condensation and caspase-3 activation in the cultured BEAS-2B suggested the death of cells by the apoptotic process.The cytotoxicityof ceria nanoparticles is mainlydue to theabsorptionaround the nuclear membrane after 1.5 h exposure [150]. Hydrothermally developed CeO_2 nanoparticles were toxic toward the prostate cancer cell lines (PC-3)revealed byMTT assay. The viability of the PC-3 cancer cells decreases to 20.19% after 72 hours of incubation with HT cerium (4+) oxide nanoparticles, which are more toxic to prostate cancer cells. In the HT method, cell viability was 88.08% higher than in the HL method for the normal mouse fibroblast cell line (L929). The nanoparticles were taken up by the cell through two processes: adhesion to the cell membrane and endocytosis by the cell. As a result, the surface charge of the particles plays an important role in the binding step[151].

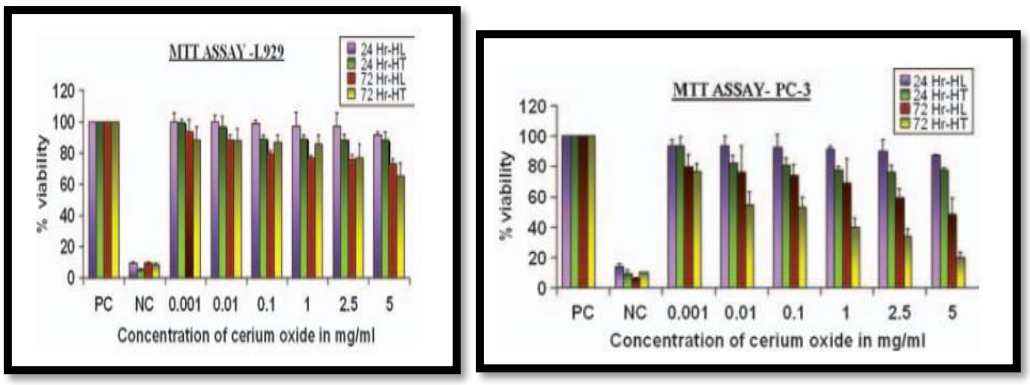

A B

Fig-11 A)Hydrothermal MTT assay cytotoxicity analysis of cerium oxide nanoparticles (HT-hydrothermal, HL-hydrolysis) after 24 and 72 hr incubation in cell line L-929 and Fig-11-B) MTT assay cytotoxicity of prostate cancer cell lines (PC-3) Ref-[151]. Copyright 2016 American Scientific Publishers

CeO_2 NPs synthesized through the sol-gel method ina gelatine medium which acts stabilizer to maintain the growth of nanostructures at low temperatures.The product wasa cubic fluorite structure of 10 nm in size.The in vitro cytotoxicity of CeO_2-NPs was measured by the MTT method on neuro-2A cells.The cellswereviable below 10 µg /mL measuredby incubating for 24 h. Thisstudy set the toxicitylevel for futureapplications in different fields[173]. The particle sizeof nanoceria showed good optical propertiesthat resulted incytotoxicity.Thecell viability of the PC-12 cancer cell linewas detected in vitro study notaffected by the nanoceria[94]and no significant toxicity was found on A549 cells prepared green method [103].

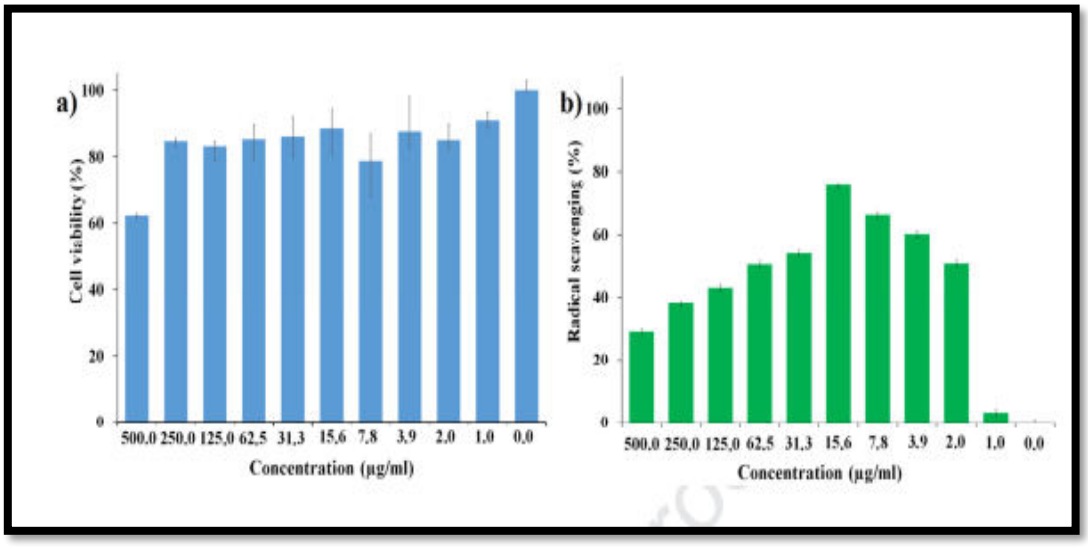

Fig.12- a)shows the percentage of cell viability versus various concentrations of CN-400. All concentrations of CN-400 indicated cell viability of more than 50%. **Fig. 12- b)** illustrates the percentage of ROS scavenging versus different

concentrations of CN-400. 15.6 µg/ml of CN-400 had the best antioxidant influence and could defuse about 76% of ROS formed by cellular metabolism. Reference-[103]

A study, reported by I.N. Bazhukova et alto prepare nanoceriathroughthe pulsed electron beam evaporation method showed cytotoxicity in four cell line dermal human fibroblasts (DHF), human embryonic kidney cells (HEK-293), human rhabdomyosarcoma (Rd), and human cervical carcinoma (HeLa) cells. The concentration of CeO_2NPs (400 µg/ml) does not affect the viability of healthy cell lines. However, the viability was decreased with an increase in the concentration of NPs [153]. M. Atif et al (2021) in their work showed that Mn-doped cerium oxide nanocomposite had remarkable cytotoxicity against the MCF-7 cancerous cells by reduction of the 68 % growth of cells. The doping increases the oxygen defects in the nanoceria and increases the ROS generation in the cell causing apoptosis resulting in cell death [154]. Fazal Abbas et al (2016) showed in their study that the Mn-doped cerianano structured sample (30-41 nm) has excellent cytotoxicity. The cytotoxicity of metal oxide depends on various parameters like particle size, electrostatic interaction between nanoparticle and cell, and the generation of reactive oxygen species (ROS).The cell viability was decreasedand directly affected the ROS production.The Mn doping in CeO_2 reduced the size of the nanoparticle to less than 20 nm which easily penetrated the cell and hurt the cell. In the second factor, various species of ROS were produced on the surface of the nanoparticles which increases the various process that leads the cell death like lipid peroxidation, apoptosis, and cell membrane damage.The pH level also plays an important role in measuring the cytotoxicity in CeO_2. The basic pH favours cell viability while the acidic pH enhances cytotoxicity.The 5 %Mn-doped sample inhibited the cell viability in cancer cells butnot in the healthy cell line, due to the production of different levels of ROS.The ROS production is directly related to cell viability. The Mn doping also enhancedthe oxygen surface defects that enhanced ROSproduction [155].A similar cytotoxicity was reported by Fazal Abbas 2017 the hydrothermally prepared Sn-doped CNP (30-50 nm)size.The sample showed anticancer activity related to the generation of ROS.The anticancer activity was performed using both HEK-293 and Neuroblastoma cells.The 5 % dopedsample showed that 40 % inhibited the cell viability in the cancer cell than the healthy HEK-293 cell.The nanoceria of smaller size is more effectivedue to band gap energies beingresponsible for the generation of ROS that cause cell death as the damageto theircellular DNA, mitochondria,cellmembrane, and plasma protein [156].Fazal Abbas et al reported that the increase in the Ni dopant concentration decreases the crystallite size of nanoparticles resulting in the enhancement of oxygen vacancies. That resultsin to increase in the ROS production on the surface of the nanoparticles. The synthesized ferromagnetic nanomaterial has different cytotoxicity against the healthy cell in comparison to the cancerous cell. The cell viability decreased in the Sh-SY5Y cancer cell line up to 55 % while in healthy

cells no such effect was observed [157]. In this study was observed that NPs prepared by the three different methods: using the NH_4OH precipitation method, NaOH precipitation, and microwave hydrothermal method, have no significant cytotoxicity against neuroblastoma cells and RAW 264.7 cells [158].

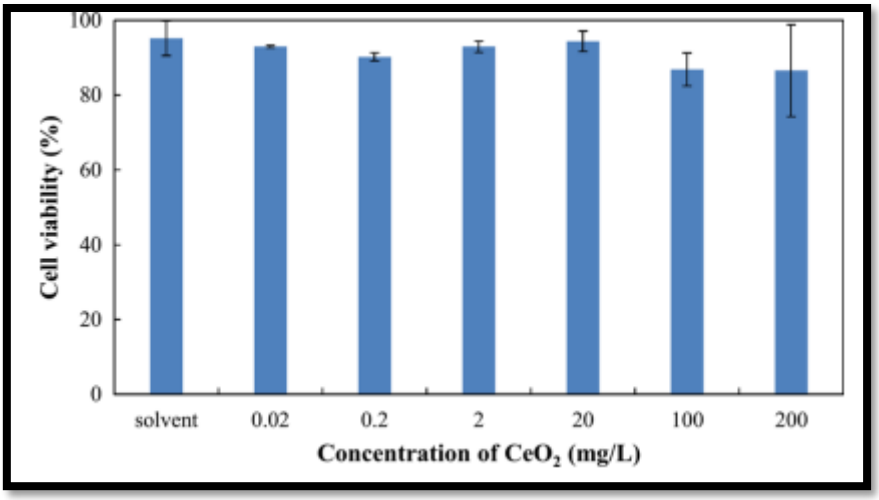

Fig-13-The cell viability of neuro-2a murine neuroblastoma cells by MTT assay under different concentrations of A-CeO2 NP through simple NH_4OH precipitation methodRef-[158].Copyright 2019Springer

Abdolhossein Miri et al 2018 studied the cytotoxicity of bio-synthesizedCeO_2 nanoparticlesthat areuniform and spherical shapedwitha 30 nm size observed againstcolon cancer cells by MTT assay.They observed the cytotoxicity of nanoceria at differentconcentrations(50,100,200,400,800 µg/ml).It was observed that no significant effect even athigh concentrationsof 800 µg/ml. According to this study, the nanoceria hasa potential biological application in various fields [159].A similar study was done byAbdolhossein Miri et al 2019 that biosynthesized nanoceria using *Salvadora persica*.The synthesized CeO_2NPs Crystallite size was 19 nm from the PXRD method and morphologywas uniform, almost spherical in shape from the FESEM image. The cytotoxicity was measured through an MTT assay against a colon HT-29 cancer cellline not show toxicity (0-800 µg/ml) range[160].

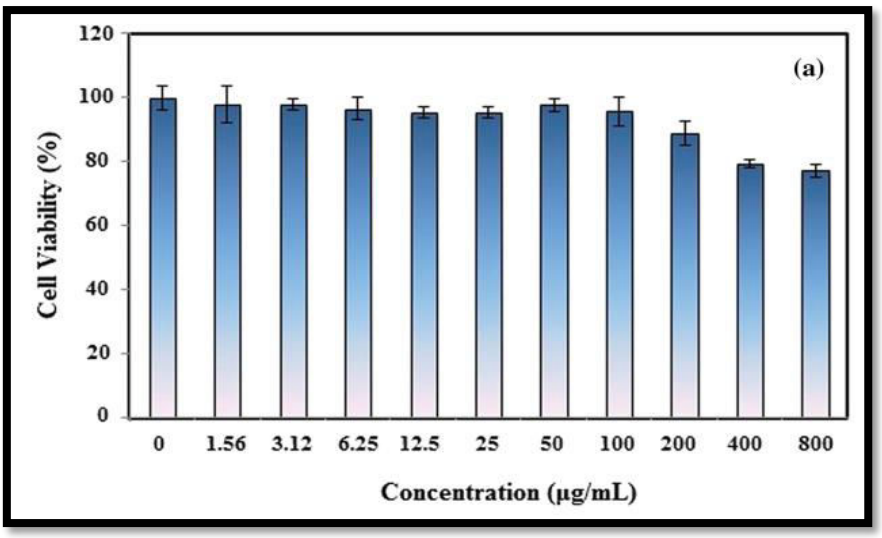

Fig .14- Represented the MTT cell viability assay of biosynthesized CeO2-NPs on HT-29 cancer cell lineswas measured at 24 h using an aqueous extract of *Salvadora persica.* Ref [160]. Copyright 2019 Wiley

The controlled size and biosynthesis of nanoceria through green synthesis using freshegg white followed by the different calcination temperatures(200,400,800 °C). The formation of nano-powder of size 25 nm, fluorite cubic structure with preferential orientation on (111) reflection plane in CeO_2.The prepared nanoparticles do not have significantcytotoxicity in the periodontal fibroblast cells inall concentrations up to 800 µg/mlin vitro study [161].Nanoceria- curcumin conjugated prepared by $CeCl_3.7H_2O$ oxidation in an alkaline medium of PVP to maintain the pH at 8.Curcumin-nanoceria conjugate was prepared under vacuum conditions in various ratios of curcumin and ceria in the range of 1:1. to 1:50 molar ratio. It showed selective cytotoxicity against the humanglioblastoma T98G cancer cell line than the normal cell line [162]. Esmail Nourmohammadi et al biosynthesised nanoceria through the carrageenan by sol-gelmethod followed by the calcination at different temperatures as 400,500,600,700and 800 ^{o} C.The surface morphology was sphericalto cylindrical with little tendency for agglomeration from SEM images.The prepared NPs do not show in-vitro cytotoxicity on the WEHI-164 cell lineeven at high concentrations up to 250 µg/ml after 24 hrs[163].Mohammad Ashna et al prepared cerium oxide (size of 25.46 nm) using pollen grains of *Brassica napus*and reported in-vitro toxicity against the human ovarian cancer cell.The concentration and the periodaffect the cell viability. The concentration of nanoceria was 12.5 µg/ml for 72 hrswhich was highly lethal to the human ovarian cancer cell line while having little effect on normal human foreskin fibroblast [164].Similar resultswere reported ofbiosynthesizednanoceria from *Ceratonia siliqua*used against thebreast cancer cell line (MCF7). The toxicity increased with treatment time and concentration of nanoceria[165] and ethanolic extract Brophyllamdaigremontianum plantused for the preparation of nanoceriaof small crystallite size and large surface area

showed excellent anticancer activity against the human breast cancer cell line MCF-7even 50 % death of cells at lower concentration of 175.04 µg/ml [166]. Nafas Abbasi et al reported that the Cerium oxide nanoparticles loaded on chitosanprepared using melon shell extract followed by the ion gelation method.The prepared sample was spherical with a size of 54.83 nmand had excellent cytotoxicity,decreasing the cell viability of cancer cells to 50 % and 97 % of the normal cells at the 50.65 µg/ml concentration of the sample.The death of cells was observed mainly due to the apoptosis process [167].A similar study done by Golnar Kermani et alrevealedhybrid nano architectonicsof Chitosan-Cerium Oxide Nanoparticlesusing rosemary leaf extract coating of chitosan around the nanoparticles by ionic gelation method.The prepared nano sample was spherical in shape with less agglomerationwith 202 .35 nm insize.The toxicity effect against 3 cancer cell lines AGS,A549, and PC3 in comparison withnormal skin fibroblast cell linesshowed.The toxicity increasedon increasing the concentration of nanoparticles.The normal cells don't show toxicity at 400 µg/ml but have high inhibitory effects onthree cancer cell lines.The main mechanism of toxicity of cells was to production ofpro-apoptotic genes therefore increasing expression of caspase 9 and 3 genes in the qPCR and increasing the SubGIcellcount confirmapoptosis in the cell.The ROS and oxidative damage are interrelated to cell death due to the apoptosis process [168].

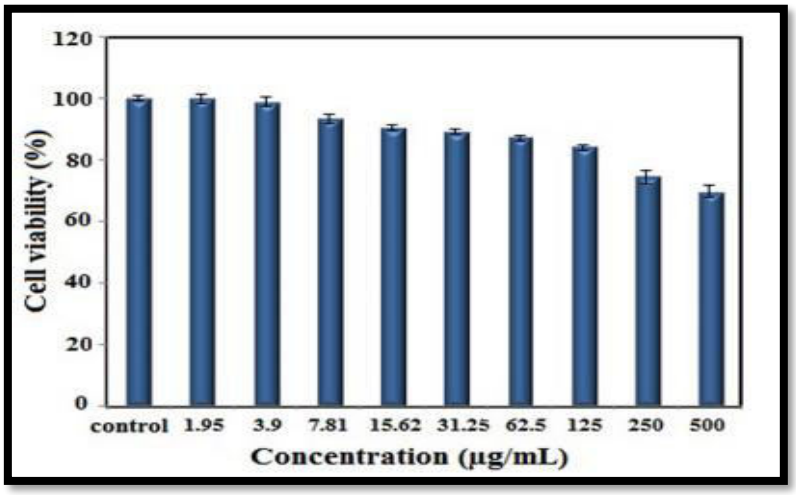

Fig.15-Cell viability of biosynthesized CeO2-NPs on A549 cell line after 24 h incubation using*Musa sapientum* peel extractRef [102]copyright 2021 Springer

3.2.3. Neurotoxicity: Neurotransmitter and neuromodulator, NO (nitric oxide) is required for the memory and the learning process. The generation of NO was mainly from the L-arginine by the action of some specific enzymes.However, the excessive production of the NO species combined with some ROS that aresuperoxide, formed peroxynitrite that was highly reactive and neurotoxic causing neuron cell death.JM Dowding 2017 in their study revealed that the nanoceria of Ce $^{+3}$ state with fluorite structure of (3-8 nm) in size. The nanoceria

prevents the Aβ or peroxynitrite production that is responsible for mitochondrial degeneration of the neuron cells.The fabricated crystalline Ag/CeO_2 nanomaterial has antibacterial activity against both bacterial strains. In this study, the Ag/CeO_2 that produces the excess amount of ROS on the surface due to the interaction with the cell wall of bacteria and nanoparticles penetrate the cell wall and kill the bacteria [111].Neuroprotectivefrom oxidative stress acts as an antioxidant to limit the production of reactive oxygen species that kill the cells [169].

Table 3 –Different approaches of cytotoxicity with theirmethods of synthesis, effects, morphology, size, and conc. of the sample

S. N	Sample	Method of Preparation	crystallite size	Particle Morphology	Cell line	Effects	Conc.of the sample	Ref.
1	CeO_2	Co-ppt (CTAB)	15.39 nm	polycrystalline nature	Human lung carcinoma cellA549	Good in-vitro anticancer activity against Human lung carcinoma cellA549 cell line	30.07 µg/ml	[86]
2	Ag-doped CeO_2	Salvia seeds extract	-	Spherical 62.7 nm	EPG 85-257 human gastric cancer cell line	No in vitro cytotoxic effects on cells up to 62.5 mM for 24 hrs after that viability of cells was decreased	62.5 mM for 24 hrs	[139]
3	CeO_2	CeO_2(+4) hydrothermal and CeO_2(+3) hydrolysis method	HT-115 nm HL-110 nm	spherical	Human prostate cancer (PC-3) and mouse fibroblast L929	HT CNPs were viability at 88.08 % and HL CNPs at 90.9 % after 24 hrs but the +3 oxidation state did not show much toxicity to the normal cell.	5 mg/L	[151]

4	Mn-CeO_2	Hydrothermal	105 nm	spherical	MCF-7 breast cancer cell line	Showed good in-vitro anticancer activity against the cancerous cell at 200 µg/ml concentration due to the ROS generation	200 µg/ml	[154]
5	Mn-doped CeO_2	Soft chemical route	6 nm	30 -41 nm spherical in shape	Neuroblastoma cancer cell and healthy cell (HEK-293 cell)	5 % Mn-doped CeO_2 inhibited the viability of 40 % of cells in the cancerous cell but no cytotoxicity towards the healthy cell.	7 % Mn-doped nanoceria are toxic to both the healthy and cancerous cells.	[155]
6	Sn-CeO_2	Hydrothermal	30-50 nm	20-30 nm spherical, beads like nanowires and nanosheets	Neuroblastoma cancer cell and normal HEK-293	Anticancer activity inhibition is 40 % but biocompatibility for healthy cells	20 µg/ml for 24 hrs	[156]
7	Ni-doped CeO_2	Soft chemical using acetic acid as a capping agent	5 nm	22 nm, spherical homogenous particle	Sh-SY5Y cancerousand healthy human cell HEK-293	Cancer cell viability reduced up to 55 % with 7 % Ni-doped CeO2 showed higher selective cytotoxicity	20 µg/ml for 24 hrs	[157]
8	CeO_2	1.NH_4OH precipitation 2.NaOH precipitation 3.	10.35 nm	12.87 nm spherical shape	Neuro 2A cells	No cytotoxicity effect on N2A cells	200 mg/L for 24 hrs	[158]

		Microwave hydrothermal						
9	CeO_2	*Prosopis farcta* aerial part extract	Less than 30 nm	uniform with Spherical in shape	HT-29 colon cancer cells line	No cytotoxicity	800 µg/ml for 24 hrs	[159]
10	CeO_2	Biosynthesis using *Salvadora persica*	19 nm	Uniform almost spherical in shape	HT-29colon cancer cells line	No cytotoxicity	800 µg/ml for 24 hrs	[160]
11	CeO_2	Fresh egg white	8-18 nm	25 nm with nanopowder of spherical shape	Human periodontal fibroblast cells	No cytotoxicity	800 µg/ml for 24 hrs	[161]
12	CeO_2	Green sol-gel method		34 nm spherical and cylindrical	WEHI-164 cell line	Not seen cytotoxicity even at 250 µg/ml concentration and metabolic activity decreased maximum at 500 µg/ml conc.	250 µg/ml	[163]
13	CeO_2	Pollen grains of *Brassica napus*	25.46 nm	23.2±4.0 nm with uniform and spherical	ovarian cancer cells (A2780)	Showed high toxicity effects on ovarian cancer cells (A2780) but little effect on normal human foreskin fibroblast cell line		[164]
14	CeO_2	Green synthesis using	22 nm	Un-uniform, spherical shape	Breast cancer cells (MCF7)	Significantly suppress the growth of the	125-250 µg/ml for 48 hrs cell	[165

		Ceratonia siliqua				cancer cells. The cytotoxicity depends on the duration of treatment and dose	viability	]
15	CeO_2	*Brophylla mdaigremontianum* plant extract	Small crystallite size	Spherical shape	Breast cancer cells (MCF7)	Cell viability decreased up to 50 % in the cancer cell line as compared to the normal L-6 cell line	175.04 µg/ml	[166]
16	CeO_2 NPs loaded on chitosan	Melon shell extract	5.69 nm	54.83nm,spherical to multifaceted	A549 cancer cell line and normal cell	High toxic to cancer cells and no toxicity towards normal cell	56.65 µg/ml for cancer cell and 131.108 µg/ml for normal cell	[167]
17	Hybrid chitosan - CeO_2	Rosemary leaf extract	202.35 nm	mono disperse, spherical with less agglomeration	AGS,A549 and PC-3 cancer cell line	showed high cytotoxicity against all cancer cells as compared to normal cell	200 µg/ml	[168]
18	Nanoceria-curcumin conjugate	Co-evaporation with (PVP)	10-15 nm	-	Human glioblastoma T98G cell line	Showed selective cytotoxicity that caused drastic inhibition of metabolic activity and decreased the total number of tumor cells.	12.5 M	[170]
19	CeO_2	Co-precipitati	5-6 nm	Uniform spherical/fl	(A549) human lung	Anticancer inhibition 40-41	400 µg/ml for 24 h	

		on and Green synthesis		ake	cancer cell	%		[171]
20	CeO_2	*Averrhoa carambola* leaf extract	24 nm	Micrographs of 5-10 µm, rock-like with uneven boundary and top surface net-like	Protest cancer(PC-3), colon cancer(HT-29) and breast cancer(MCF-7) cell line	CeO_2 NPs showed more cytotoxicity against the breast cancer(MCF-7) than Protest cancer(PC-3), colon cancer(HT-29) cell lines	20 µg/ml for 72 hrs	[172]
21	CeO_2	Green synthesis	22 nm	15-20 nm	Colon cancer cell lines (HT-29)	No cytotoxic effect 400 µg/ml for 24 hrs	Cell viability 58.2 % in 500 µg/ml	[173]
22	Cd-Doped(1 &5%) and undoped CeO_2	Green synthesis using *Salvadora persica*	8.33, 11.91 .18.94 nm	15-20 nm uniform and almost spherical shape	Brest cancer (MCF-7) cell line	Cell viability was decreased by increasing the concentration of Cd to CeO_2 NPs. And reduced the cell viability by 50 %	-	[174]
23	Mg-doped CeO_2	*Hibiscus sabdarifa*	100 nm size due to the presence of Mg	orbicular	HepG-2 (Hepatocellular carcinoma cells), MCF-7(Breast carcinoma cells), and A-549 (Lung carcinoma cells).	Biosynthesize Mg-doped acts as an excellent anticancer activity against the three cancer cell lines. The higher toxicity was observed in A-549 cells with IC_{50}=79.19 ± 3.07 µg/mL and maximum cell inhibition of	109.65 ± 4.13 µg/ mL (HepG2) 113.55 ± 3.89 µg/mL (MCF-7) and 79.19 ± 3.07 µg/mL	[175]

						almost 96 %		
24.	CeO_2 NPs	*Falcaria Vulgaris* leaf extract	19.5 nm	mostly spherical	PC3 Human prostate cancer cancer cells.	Cell viability and real-time PCR tests confirmed that the biosynthesized CeO2 NPs suppress cell metastasis of the cancer cells, and enhance cell cycle arrest and apoptosis in the cancer cells.	113.6 μg/mL after 24 h treatment.	[176]
25.	CeO_2 NPs	Green synthesis using Carrageenan	34 nm	spherical shape	WEHI 164 cancer cell line	In-vitro cytotoxicity effects of biosynthesized CeO2 NPs with the WEHI 164 cancer cell showed no cytotoxicity in the range of 0-500 and a maximum decrease in cell metabolic activity at 500 μg/ml	0-500 μg/mL after 24 h	[177]

Antioxidant Properties: The antioxidant species are generated by the oxidation process of theorganic compoundsas lipids, proteins, nuclear acids,and proteins.The ROS represents the hydroxyl OH·and O_2·superoxide radicals, H_2O_2hydrogen peroxide, and NO·radicals. These species are very reactive and cause damage to the cells and toxic effects.The presence of these ROS caused oxidative stress and induced cell death.Nitricoxide is one of the important ROS that cause the inflammatory process in the cell.The cerium NPs prepared by the solvothermal method have excellent free radicals scavenging ability.In vitro,studiesshowed good free radicalscavenging activity for both NO and DPPH. Both nanomaterials of ceria show 55 % antioxidant activity at 75 mg ml^{-1}

concentration inthe DPPH assay[178].Another study confirms that nanoceria synthesized by simple wet chemical method nanoparticles are agglomerated with clusters of size between 5-50 nm.The prepared nanoceria suppresses the ROS production that protects the cells.The flow cytometry test measured the nanoceriascavenging propertyof free radicalnitric oxide in J774A.1macrophage[179]. It has been reported thatPectin-mediated synthesized nanoceria showed a DPPH radical scavengingcapacity was 73.36 % in 60 min at the 4.0 mg/mL concentration of nanoceria.Due to this property, they showed very good antibacterial activity against gram-negative bacteriathan gram-positive bacteria[180].In this study,the CeO_2wassynthesizedthroughprecipitation using the mixed water-alcohol solution at constant pH = 9.The size of nanoparticles variesfrom 14to 4.2 nmwith the decrease in size on increasing the concentration of alcohol.Theantioxidant activity was determinedintwo ways: i) in-vitro antioxidant activity was tested against on-cell line; ii) antioxidant property as the nano enzyme that acts as the pseudo enzyme i.e. catalase and superoxide dismutase-like behavior [181].Greensynthesized nanoceria from *Ceratonia siliqua* extract with an average sizeof 22 nm showed antioxidant properties.The antioxidant properties increase with the concentration ofnanoparticles.The low Ce^{+3}/Ce^{+4}surface ratioaffects the antioxidant catalase-mimetics activity of nanoparticles.The antioxidant properties of CeO_2NPs were investigated through the DPPH test.The prepared nanomaterials have excellent free radical scavenging capabilities than the BHA.CeO_2NPs are capable of removing DPPH radicals in a concentration-dependent by increasing the concentration of nanoparticles increasing the antioxidant property [165].The antioxidant activity of prepared CeO_2 NPs (33.31 nm) crystallite size showed a strong peak at 521 cm-1 in Raman spectra due to the oxygen vacancy. The surface morphologyshowshigh homogeneity with a spherical shape of average diameter 60-85.1 nm. TheCeO_2NPs have excellent scavenging capabilities. The low surface ratio of Ce^{+3}/Ce^{+4} on CeO_2NPs acts as an efficient antioxidant catalyseenzyme property. The proton-donating capacity of CeO_2NPsprevents the generation of free radicals and this property increases with the concentration of the NPs [182].Tuning the morphology of nanoceria was prepared by thermal decomposition of cerium nitrate using capping agent octylamine or oleylamine at two different temperatures. The capping agent and temperature affect nanoparticle properties like size, morphology, agglomeration, and Ce^{+3}/Ce^{+4} ratio. The antioxidant property of prepared nanoparticles was evaluated on the HaCaT human cells.The production of ROS was inhibited against the sodium arsenite (SA) induced oxidative stress [183].Sushant et al in their study reported thatCeO_2 NPs can act as regenerative ROS scavengers. It acts as the SOD or catalase mimetic activity. These activities mainly depend on the surface ratio of the Ce^{+3}/Ce^{+4} valency state.CeO_2 NPs showed SOD activity when Ce^{+3} (62 %)was higher than Ce^{+4}(38 %)and also on the concentration and catalase mimetic when Ce^{+4}[184]. Debanjan Dutta et al in this study resolve the contradictory behavior of nanoceria as toxic

and nontoxic properties respectively.The nanoceria act as toxic whenthe Ce^{+3}/Ce^{+4} ratio is higher.The toxicity of NPs was mainly due to the Ce^{+3}which acts as a strong oxidizing agent.It easily donated its $4f^1$ electro to the periphery atom and attained the Ce^{+4} oxidation state that was more stable because of the inert gas configuration.But in the presence of oxidative stress, the Ce^{+3} higher ratio causes the antioxidant property against the ROS and appears to be highly protective in nature [185].

Conclusion

In this review article, different methods of preparationhave been discussed that have been used for the synthesis of nanoceria. The characterization and effective uses in the different fields like photocatalyst, sensor, and biomedical applications. Several chemical methods like hydrothermal, co-precipitation, microwave, wet chemical, and green methods of synthesis are very important methods to prepare nanoceria. The physicochemical properties that are directly affectedby the production of ROSare responsible for the various properties in the developed Ceria NPs.Among the various chemical methods are effective but the green method approach has more advantages of synthesis as found to be eco-friendlier and more economical.This kind of synthesis approach can save time, and cost, whichproduces nanoceria of smaller size that are effective fields. The various factors like reaction time, pH of the reaction, different precursors, solvents, heating time, and temperature can also enhance the applications of nanoceria.The cerium oxide nanoparticles showed potential applications in the biological fields. They showed anticancer, antioxidant, anti-inflammatory, and antimicrobial activity. The biological properties of nanoceria are mainly due to the existence of two oxidant states, Ce+3 and Ce+4.The doping affects the shape, size, and morphology of the nanoceria which directly affects the photocatalytic activity of the catalyst.The size and the surface area of the nanoparticles play an important role in the photodegradation activity.The presence of plenty of oxygen vacancy is also responsible for the photocatalytic degradation of dye. These oxygen vacancies in the nanoceria lattice which is the main source of adsorption of water molecules, act as the active sites for the water dissociation. The green synthesized nanoceria showed excellent biological activity than the chemically prepared nanoceria.

Author Address:

[1]Department of Chemistry D.P.D.B.H. Govt (PG) College Kotdwar Pauri Garhwal, Uttarakhand, India

[2]Department of Chemistry Govt. Degree College Rudrasaprayag,Uttarakhand, India

[3]Department of Chemistry School of Applied and Life Sciences Uttaranchal University Dehradun, India

[4]Department of Botany, Chinmaya Degree College, BHEL, HARIDWAR, Uttarakhand, India
[5]DBS School of Pharmacy and Research, [5]DBS Global University, Dehradun, Uttarakhand, India
[6]Department of Botany, Hari Om Saraswati P.G. College, Dhanauri, Haridwar, Uttarakhand, India
[7]Smt. Mohari Devi Taparia Kanya Mahavidhyalaya, Jaswanthgarh, Rajasthan.
[8]Department of Pharmaceutical Sciences, Gurukula Kangri (Deemed to be University) Haridwar, Uttarakhand, India

References

- Bear, J. C., Yu, B., Blanco-Andujar, C., McNaughter, P. D., Southern, P., Mafina, M. K., ... & Parkin, I. P. (2014). A low-cost synthesis method for functionalised iron oxide nanoparticles for magnetic hyperthermia from readily available materials. Faraday Discussions, 175, 83-95.
- Na, H. B., Lee, J. H., An, K., Park, Y. I., Park, M., Lee, I. S., ... & Hyeon, T. (2007). Development of a T1 contrast agent for magnetic resonance imaging using MnO nanoparticles. Angewandte Chemie, 119(28), 5493-5497.
- Varga, E., Pusztai, P., Óvári, L., Oszkó, A., Erdőhelyi, A., Papp, C., ... & Kiss, J. (2015). Probing the interaction of Rh, Co and bimetallic Rh–Co nanoparticles with the CeO 2 support: Catalytic materials for alternative energy generation. Physical Chemistry Chemical Physics, 17(40), 27154-27166.
- Motaghi, S., & Farahmandjou, M. (2019). Structural and optoelectronic properties of Ce–Al2O3 nanoparticles prepared by sol-gel precursors. Materials Research Express, 6(4), 045008.
- Masui, T., Hirai, H., Hamada, R., Imanaka, N., Adachi, G. Y., Sakata, T., & Mori, H. (2003). Synthesis and characterization of cerium oxide nanoparticles coated with turbostratic boron nitride. Journal of Materials Chemistry, 13(3), 622-627.
- Gnanam, S., & Rajendran, V. (2011). Synthesis of CeO 2 or α–Mn 2 O 3 nanoparticles via sol–gel process and their optical properties. Journal of sol-gel science and technology, 58, 62-69.
- Riwotzki, K., Meyssamy, H., Kornowski, A., & Haase, M. (2000). Liquid-phase synthesis of doped nanoparticles: colloids of luminescing LaPO4: Eu and CePO4: Tb particles with a narrow particle size distribution. The Journal of Physical Chemistry B, 104(13), 2824-2828.
- Masalov, A., Viagin, O., Maksimchuk, P., Seminko, V., Bespalova, I., Aslanov, A., ... & Zorenko, Y. (2014). Formation of luminescent centers in CeO2 nanocrystals. Journal of luminescence, 145, 61-64.

- Ho, C., Yu, J. C., Kwong, T., Mak, A. C., & Lai, S. (2005). Morphology-controllable synthesis of mesoporous CeO2 nano-and microstructures. Chemistry of Materials, 17(17), 4514-4522.
- Malleshappa, J., Nagabhushana, H., Sharma, S. C., Vidya, Y. S., Anantharaju, K. S., Prashantha, S. C., ... & Surendra, B. S. (2015). Leucas aspera mediated multifunctional CeO2 nanoparticles: structural, photoluminescent, photocatalytic and antibacterial properties. Spectrochimica Acta Part A: Molecular and Biomolecular Spectroscopy, 149, 452-462. doi:
- Malleshappa, J., Nagabhushana, H., Sharma, S. C., Vidya, Y. S., Anantharaju, K. S., Prashantha, S. C., ... & Surendra, B. S. (2015). Leucas aspera mediated multifunctional CeO2 nanoparticles: structural, photoluminescent, photocatalytic and antibacterial properties. Spectrochimica Acta Part A: Molecular and Biomolecular Spectroscopy, 149, 452-462.
- Maheswari, N., & Muralidharan, G. (2015). Supercapacitor behavior of cerium oxide nanoparticles in neutral aqueous electrolytes. Energy & Fuels, 29(12), 8246-8253.
- Sunqing, Q., Junxiu, D., & Guoxu, C. (1999). Tribological properties of CeF3 nanoparticles as additives in lubricating oils. Wear, 230(1), 35-38.
- . Mohanty, B., Chattopadhyay, A., & Nayak, J. (2021). Band gap engineering and enhancement of electrical conductivity in hydrothermally synthesized CeO2–PbS nanocomposites for solar cell applications. Journal of Alloys and Compounds, 850, 156735.
- García, A., Delgado, L., Torà, J. A., Casals, E., González, E., Puntes, V., ... & Sánchez, A. (2012). Effect of cerium dioxide, titanium dioxide, silver, and gold nanoparticles on the activity of microbial communities intended in wastewater treatment. Journal of hazardous materials, 199, 64-72.
- Dahle, J. T., & Arai, Y. (2015). Environmental geochemistry of cerium: applications and toxicology of cerium oxide nanoparticles. International journal of environmental research and public health, 12(2), 1253-1278.
- Krishnamoorthy, K., Veerapandian, M., Zhang, L. H., Yun, K., & Kim, S. J. (2014). Surface chemistry of cerium oxide nanocubes: Toxicity against pathogenic bacteria and their mechanistic study. Journal of Industrial and Engineering Chemistry, 20(5), 3513-3517.
- Hedrick, J. B., & Sinha, S. P. (1994). Cerium-based polishing compounds: discovery to manufacture. Journal of alloys and compounds, 207, 377-382.
- Liu, X., Yin, S., & Sato, T. (2009, February). Synthesis and UV-shielding characterization of plate-like titanate/calcia-doped ceria composite. In IOP Conference Series: Materials Science and Engineering (Vol. 1, No. 1, p. 012013). IOP Publishing.

- Onoda, H., & Tanaka, R. (2019). Synthesis of cerium phosphate white pigments from cerium carbonate for cosmetics. Journal of Materials Research and Technology, 8(6), 5524-5528.
- Zholobak, N. M., Shcherbakov, A. B., Bogorad-Kobelska, A. S., Ivanova, O. S., Baranchikov, A. Y., Spivak, N. Y., & Ivanov, V. K. (2014). Panthenol-stabilized cerium dioxide nanoparticles for cosmeceutic formulations against ROS-induced and UV-induced damage. Journal of Photochemistry and Photobiology B: Biology, 130, 102-108.
- Chen, Y., Qiu, C., Chen, C., Fan, X., Xu, S., Guo, W., & Wang, Z. (2014). Facile synthesis of ceria nanospheres by Ce (OH) CO3 precursors. Materials Letters, 122, 90-93.
- Dao, N. N., Luu, M. D., Nguyen, Q. K., & Kim, B. S. (2011). UV absorption by cerium oxide nanoparticles/epoxy composite thin films. Advances in Natural Sciences: Nanoscience and Nanotechnology, 2(4), 045013.
- Khan, M., Mashwani, Z. U. R., Ikram, M., Raja, N. I., Mohamed, A. H., Ren, G., & Omar, A. A. (2022). Efficacy of green cerium oxide nanoparticles for potential therapeutic applications: Circumstantial insight on mechanistic aspects. Nanomaterials, 12(12), 2117.
- Montini, T., Melchionna, M., Monai, M., & Fornasiero, P. (2016). Fundamentals and catalytic applications of CeO2-based materials. Chemical reviews, 116(10), 5987-6041.
- Garzon, F. H., Mukundan, R., & Brosha, E. L. (2000). Solid-state mixed potential gas sensors: theory, experiments and challenges. Solid State Ionics, 136, 633-638.
- Vigneselvan, S., Manikandan, V., Petrila, I., Vanitha, A., & Chandrasekaran, J. (2020). Effect of copper substitution on structural, optical and humidity-sensing characteristics of cerium oxide nanoparticles. Journal of Physics and Chemistry of Solids, 136, 109173.
- Thakur, S., & Patil, P. (2014). Rapid synthesis of cerium oxide nanoparticles with superior humidity-sensing performance. Sensors and Actuators B: Chemical, 194, 260-268.
- Mazur, F., Han, Z., Tjandra, A. D., & Chandrawati, R. (2024). Digitalization of colorimetric sensor technologies for food safety. Advanced Materials, 36(42), 2404274.
- Subbiah, D. K., Kulandaisamy, A. J., George, R. B., Shankar, P., Mani, G. K., Babu, K. J., & Rayappan, J. B. B. (2018). Nano ceria as xylene sensor–Role of cerium precursor. Journal of Alloys and Compounds, 753, 771-780.
- Qian, J., Wang, Y., Pan, J., Chen, Z., Wang, C., Chen, J., & Wu, Z. (2020). Non-enzymatic glucose sensor based on ZnO–CeO2 whiskers. Materials Chemistry and Physics, 239, 122051.

- Kim, N. W., Lee, D. K., & Yu, H. (2019). Selective shape control of cerium oxide nanocrystals for photocatalytic and chemical sensing effect. RSC advances, 9(24), 13829-13837.
- Liao, L., Mai, H. X., Yuan, Q., Lu, H. B., Li, J. C., Liu, C., ... & Yu, T. (2008). Single CeO2 nanowire gas sensor supported with Pt nanocrystals: gas sensitivity, surface bond states, and chemical mechanism. The Journal of Physical Chemistry C, 112(24), 9061-9065.
- Allasi, H. L., Rajalingam, A. A., Jani, S. P., & Uppalapati, S. (2023). Influence of synthesized (green) cerium oxide nanoparticle with neem (Azadirachta indica) oil biofuel. Bulletin of the Chemical Society of Ethiopia, 37(2), 477-490.
- González-Mancebo, D., Becerro, A. I., Rojas, T. C., Olivencia, A., Corral, A., Balcerzyk, M., ... & Ocaña, M. (2018). Room temperature synthesis of water-dispersible Ln3+: CeF3 (Ln= Nd, Tb) nanoparticles with different morphology as bimodal probes for fluorescence and CT imaging. Journal of Colloid and Interface Science, 520, 134-144.
- Arunachalam, T., Karpagasundaram, M., & Rajarathinam, N. (2017). Ultrasound assisted green synthesis of cerium oxide nanoparticles using Prosopis juliflora leaf extract and their structural, optical and antibacterial properties. Materials Science-Poland, 35(4), 791-798.
- Muthuvel, A., Jothibas, M., Manoharan, C., & Jayakumar, S. J. (2020). Synthesis of CeO 2-NPs by chemical and biological methods and their photocatalytic, antibacterial and in vitro antioxidant activity. Research on Chemical Intermediates, 46, 2705-2729
- Bartůněk, V., Rak, J., Král, V., & Smrčková, O. (2011). Simple one-step preparation of cerium trifluoride nanoparticles. Journal of Fluorine Chemistry, 132(4), 298-301.
- Sun, C., Li, H., Zhang, H., Wang, Z., & Chen, L. (2005). Controlled synthesis of CeO2 nanorods by a solvothermal method. Nanotechnology, 16(9), 1454.
- Hewer, T. L., Soeira, L. S., Brito, G. E., & Freire, R. S. (2013). One-pot green synthesis of cerium oxide–carbon microspheres and their catalytic ozonation activity. Journal of Materials Chemistry A, 1(20), 6169-6174 .
- Bear, J. C., McNaughter, P. D., Southern, P., O'Brien, P., & Dunnill, C. W. (2015). Nickel-doped ceria nanoparticles: the effect of annealing on room temperature ferromagnetism. Crystals, 5(3), 312-326.
- Ivanov, V. K., Shcherbakov, A. B., & Usatenko, A. V. (2009). Structure-sensitive properties and biomedical applications of nanodispersed cerium dioxide. Russian chemical reviews, 78(9), 855.
- An, K., Long, C., Sui, Y., Qing, Y., Zhao, G., An, Z., ... & Liu, C. (2020). Large-scale preparation of superhydrophobic cerium dioxide

nanocomposite coating with UV resistance, mechanical robustness, and anti-corrosion properties. Surface and Coatings Technology, 384, 125312.

- Fu, Y. P., Wen, S. B., & Lu, C. H. (2008). Preparation and characterization of samaria-doped ceria electrolyte materials for solid oxide fuel cells. Journal of the American Ceramic Society, 91(1), 127-131.
- Ecco, L. G., Rossi, S., Deflorian, F., & Fedel, M. (2018). Colloidal cerium oxide nanoparticles: preparation and corrosion inhibition performance on AA5005 aluminum alloy. Journal of The Electrochemical Society, 165(2), C86.
- Elahi, B., Mirzaee, M., Darroudi, M., Oskuee, R. K., Sadri, K., & Amiri, M. S. (2019). Preparation of cerium oxide nanoparticles in Salvia Macrosiphon Boiss seeds extract and investigation of their photo-catalytic activities. Ceramics International, 45(4), 4790-4797.
- Cao, W., Ju, P., Wang, Z., Zhang, Y., Zhai, X., Jiang, F., & Sun, C. (2020). Colorimetric detection of H2O2 based on the enhanced peroxidase mimetic activity of nanoparticles decorated Ce2 (WO4) 3 nanosheets. Spectrochimica Acta Part A: Molecular and Biomolecular Spectroscopy, 239, 118499.
- Kumar, S., Ojha, A. K., Patrice, D., Yadav, B. S., & Materny, A. (2016). One-step in situ synthesis of CeO 2 nanoparticles grown on reduced graphene oxide as an excellent fluorescent and photocatalyst material under sunlight irradiation. Physical Chemistry Chemical Physics, 18(16), 11157-11167.
- Cuahtecontzi-Delint, R., Mendez-Rojas, M. A., Bandala, E. R., Quiroz, M. A., Recillas, S., & Sanchez-Salas, J. L. (2013). Enhanced antibacterial activity of CeO2 nanoparticles by surfactants. International Journal of Chemical Reactor Engineering, 11(2), 781-785.
- Lin, K. S., & Chowdhury, S. (2010). Synthesis, characterization, and application of 1-D cerium oxide nanomaterials: a review. International journal of molecular sciences, 11(9), 3226-3251.
- Dos Santos, M. L., Lima, R. C., Riccardi, C. S., Tranquilin, R. L., Bueno, P. R., Varela, J. A., & Longo, E. (2008). Preparation and characterization of ceria nanospheres by microwave-hydrothermal method. Materials Letters, 62(30), 4509-4511.
- Gao, F., Lu, Q., & Komarneni, S. (2006). Fast synthesis of cerium oxide nanoparticles and nanorods. Journal of nanoscience and nanotechnology, 6(12), 3812-3819.
- Ji, Z., Wang, X., Zhang, H., Lin, S., Meng, H., Sun, B., ... & Zink, J. I. (2012). Designed synthesis of CeO2 nanorods and nanowires for studying toxicological effects of high aspect ratio nanomaterials. ACS nano, 6(6), 5366-5380.
- Bugayeva, N., & Robinson, J. (2007). Synthesis of hydrated CeO2 nanowires and nanoneedles. Materials science and technology, 23(2), 237-241.

- Zarinkamar, M., Farahmandjou, M., & Firoozabadi, T. P. (2016). One-step synthesis of ceria (CeO2) nano-spheres by a simple wet chemical method. Journal of Ceramic Processing Research, 17(3), 166-169. www.researchgate.net
- Hirano, M., & Kato, E. (1999). Hydrothermal synthesis of nanocrystalline cerium (IV) oxide powders. Journal of the American Ceramic Society, 82(3), 786-788.
- Zhang, Y., Kang, Z., Dong, J., Abernathy, H., & Liu, M. (2006). Self-assembly of cerium compound nanopetals via a hydrothermal process: Synthesis, formation mechanism and properties. Journal of Solid State Chemistry, 179(6), 1733-1738.
- Masui, T., Hirai, H., Imanaka, N., Adachi, G., Sakata, T., & Mori, H. (2002). Synthesis of cerium oxide nanoparticles by hydrothermal crystallization with citric acid. Journal of Materials Science Letters, 21, 489-491.
- Chen, H. I., & Chang, H. Y. (2004). Homogeneous precipitation of cerium dioxide nanoparticles in alcohol/water mixed solvents. Colloids and Surfaces A: Physicochemical and Engineering Aspects, 242(1-3), 61-69.
- Chen, H. I., & Chang, H. Y. (2005). Synthesis of nanocrystalline cerium oxide particles by the precipitation method. Ceramics International, 31(6), 795-802.
- Yin, L., Wang, Y., Pang, G., Koltypin, Y., & Gedanken, A. (2002). Sonochemical synthesis of cerium oxide nanoparticles—effect of additives and quantum size effect. Journal of Colloid and Interface Science, 246(1), 78-84.
- Pinjari, D. V., & Pandit, A. B. (2011). Room temperature synthesis of crystalline CeO2 nanopowder: advantage of sonochemical method over conventional method. Ultrasonics sonochemistry, 18(5), 1118-1123.
- Li, Y. X., Chen, W. F., Zhou, X. Z., Gu, Z. Y., & Chen, C. M. (2005). Synthesis of CeO2 nanoparticles by mechanochemical processing and the inhibiting action of NaCl on particle agglomeration. Materials Letters, 59(1), 48-52.
- Hu, C., Zhang, Z., Liu, H., Gao, P., & Wang, Z. L. (2006). Direct synthesis and structure characterization of ultrafine CeO2 nanoparticles. Nanotechnology, 17(24), 5983.
- Gu, H., & Soucek, M. D. (2007). Preparation and characterization of monodisperse cerium oxide nanoparticles in hydrocarbon solvents. Chemistry of Materials, 19(5), 1103-1110.
- Bumajdad, A., Eastoe, J., & Mathew, A. (2009). Cerium oxide nanoparticles prepared in self-assembled systems. Advances in colloid and interface science, 147, 56-66.
- Zeljković, S., Jelić, D., Maruyama, H., & Nino, J. C. (2019). Solvent-deficient synthesis of cerium oxide: Characterization and kinetics. Ceramics International, 45(8), 10063-10071.

- Chelliah, M., Rayappan, J. B. B., & Krishnan, U. M. (2012). Synthesis and characterization of cerium oxide nanoparticles by hydroxide mediated approach. Journal of Applied Sciences, 12(16), 1734-1737..
- Lakhotia, S. R., Mukhopadhyay, M., & Kumari, P. (2018). Cerium oxide nanoparticles embedded thin-film nanocomposite nanofiltration membrane for water treatment. Scientific reports, 8(1), 4976.
- Huang, P. X., Wu, F., Zhu, B. L., Gao, X. P., Zhu, H. Y., Yan, T. Y., ... & Song, D. Y. (2005). CeO2 nanorods and gold nanocrystals supported on CeO2 nanorods as catalyst. The Journal of Physical Chemistry B, 109(41), 19169-19174.
- Swetha, B., Julian, O., Shashank, S., Nicholas, E., Rameech, M., Soumen, D., ... & Sudipta, S. (2017). Modulating the Catalytic Activity of Cerium Oxide Nanoparticles with the Anion of the Precursor Salt. pubs.acs.org on August 22, 2017.
- Wang, W., Howe, J. Y., Li, Y., Qiu, X., Joy, D. C., Paranthaman, M. P., ... & Gu, B. (2010). A surfactant and template-free route for synthesizing ceria nanocrystals with tunable morphologies. Journal of Materials Chemistry, 20(36), 7776-7781.
- Reshma, P., & Ashwini, K. (2017). Cerium Oxide Nanoparticles: Synthesis, Characterization and Study of Antimicrobial Activity. J Nanomater Mol Nanotechnol 6: 3. of, 4, 1-4.
- Cui, R., Lu, W., Zhang, L., Yue, B., & Shen, S. (2009). Template-free synthesis and self-assembly of CeO2 nanospheres fabricated with foursquare nanoflakes. The Journal of Physical Chemistry C, 113(52), 21520-21525.
- Abbas, F., Iqbal, J., Jan, T., Badshah, N., Mansoor, Q., & Ismail, M. (2016). Structural, morphological, Raman, optical, magnetic, and antibacterial characteristics of CeO 2 nanostructures. International Journal of Minerals, Metallurgy, and Materials, 23, 102-108.
- Sehar, S., Naz, I., Rehman, A., Sun, W., Alhewairini, S. S., Zahid, M. N., & Younis, A. (2021). Shape-controlled synthesis of cerium oxide nanoparticles for efficient dye photodegradation and antibacterial activities. Applied Organometallic Chemistry, 35(1), e6069.
- Ghahramani, Z., Arabi, A. M., Shafiee Afarani, M., & Mahdavian, M. (2020). Solution combustion synthesis of cerium oxide nanoparticles as corrosion inhibitor. International Journal of Applied Ceramic Technology, 17(3), 1514-1521.
- Divya, T., Anjali, C., Sunajadevi, K. R., Anas, K., & Renuka, N. K. (2021). Influence of hydrothermal synthesis conditions on lattice defects in cerium oxide. Journal of Solid State Chemistry, 300, 122253.
- Mazhar, M. E., Bakhtawar, S., Rana, A. M., Usmani, M. N., Akhtar, N., Abbas, W., ... & Ahmad, J. (2019). Insight into the structural

characterization of pure and Zr-doped hydrothermally synthesized cerium oxide nanoparticles. Materials Research Express, 6(10), 105022.

- Dos Santos, A. P. B., Dantas, T. C. M., Costa, J. A. P., Souza, L. D., Soares, J. M., Caldeira, V. P. S., ... & Santos, A. G. D. (2020). Formation of CeO2 nanotubes through different conditions of hydrothermal synthesis. Surfaces and Interfaces, 21, 100746.
- Khadar, Y. S., Balamurugan, A., Devarajan, V. P., & Subramanian, R. (2017). Hydrothermal synthesis of gadolinium (Gd) doped cerium oxide (CeO2) nanoparticles: characterization and antibacterial activity. Oriental Journal of Chemistry, 33(5), 2405.
- Dhannia, T., Jayalekshmi, S., Kumar, M. S., Rao, T. P., & Bose, A. C. (2009). Effect of aluminium doping and annealing on structural and optical properties of cerium oxide nanocrystals. Journal of Physics and Chemistry of Solids, 70(11), 1443-1447.
- Dhannia, T., Jayalekshmi, S., Kumar, M. S., Rao, T. P., & Bose, A. C. (2010). Effect of iron doping and annealing on structural and optical properties of cerium oxide nanocrystals. Journal of Physics and Chemistry of Solids, 71(7), 1020-1025.
- Farahmandjou, M., & Dastpak, M. (2018). Fe-Loaded CeO2 nanosized prepared by simple Co-precipitation route. Physical Chemistry Research, 6(4), 713-720.
- Renuka, N. K. (2012). Structural characteristics of quantum-size ceria nano particles synthesized via simple ammonia precipitation. Journal of Alloys and Compounds, 513, 230-235.
- Pathak, V., Lad, P., Thakkar, A. B., Thakor, P., Deshpande, M. P., & Pandya, S. (2023). Synthesis, characterization and applications of cubic fluorite cerium oxide nanoparticles: a comprehensive study. Results in Surfaces and Interfaces, 11, 100111.
- Aseena, S., Abraham, N., & Babu, V. S. (2023). Morphological and optical studies of zinc doped cerium oxide nanoparticles prepared by single step co-precipitation method. Materials Today: Proceedings, 80, 1901-1905.
- Ramachandran, M., Subadevi, R., & Sivakumar, M. (2019). Role of pH on synthesis and characterization of cerium oxide (CeO2) nano particles by modified co-precipitation method. Vacuum, 161, 220-224.
- Channei, D., Nakaruk, A., Jannoey, P., & Phanichphant, S. (2019). Preparation and characterization of Pd modified CeO2 nanoparticles for photocatalytic degradation of dye. Solid State Sciences, 87, 9-14.
- Soren, S., Bessoi, M., & Parhi, P. (2015). A rapid microwave initiated polyol synthesis of cerium oxide nanoparticle using different cerium precursors. Ceramics International, 41(6), 8114-8118.

- Kumar, E., Selvarajan, P., & Muthuraj, D. (2013). Synthesis and characterization of CeO2 nanocrystals by solvothermal route. Materials Research, 16, 269-276.
- Parvathy, S., & Venkatraman, B. R. (2017). Synthesis and characterization of various metal ions doped CeO2 nanoparticles derived from the Azadirachta indica leaf extracts. Chemical Science Transactions, 6(4), 513-522.
- Gopinath, K., Karthika, V., Sundaravadivelan, C., Gowri, S., & Arumugam, A. (2015). Mycogenesis of cerium oxide nanoparticles using Aspergillus niger culture filtrate and their applications for antibacterial and larvicidal activities. Journal of Nanostructure in Chemistry, 5, 295-303.
- Sabouri, Z., Sabouri, M., Amiri, M. S., Khatami, M., & Darroudi, M. (2022). Plant-based synthesis of cerium oxide nanoparticles using Rheum turkestanicum extract and evaluation of their cytotoxicity and photocatalytic properties. Materials Technology, 37(8), 555-568.
- Kalaycıoğlu, Z., Geçim, B., & Erim, F. B. (2022). Green synthesis of cerium oxide nanoparticles from turmeric and kinds of honey: characterisations, antioxidant and photocatalytic dye degradation activities. Advances in Natural Sciences: Nanoscience and Nanotechnology, 13(1), 015016.
- Das, S., Panicker, N. J., Rather, M. A., Mandal, M., & Sahu, P. P. (2022). Green synthesis of cerium oxide nanoparticles using Dillenia indica aqueous extract and its anti-oxidant activity. Bulletin of Materials Science, 46(1), 3.
- Muthuvel, A., Jothibas, M., Mohana, V., & Manoharan, C. J. I. C. C. (2020). Green synthesis of cerium oxide nanoparticles using Calotropis procera flower extract and their photocatalytic degradation and antibacterial activity. Inorganic Chemistry Communications, 119, 108086.
- Kaygusuz, H., & Erim, F. B. (2020). Biopolymer-assisted green synthesis of functional cerium oxide nanoparticles. Chemical Papers, 74(7), 2357-2363.
- Irshad, M. S., Aziz, M. H., Fatima, M., Rehman, S. U., Idrees, M., Rana, S., ... & Huang, Q. (2019). Green synthesis, cytotoxicity, antioxidant and photocatalytic activity of CeO2 nanoparticles mediated via orange peel extract (OPE). Materials Research Express, 6(9), 0950a4.
- Gunasekaran, N. K., Tumkur, P. P., Bayon, N. N., Prabhakaran, K., Arasho, W. D., Hall, J. C., & Ramesh, G. T. (2023). Cerium Oxide Nanoparticles: Synthesis and Characterization Using Curcuma longa (Turmeric Rhizome). Energy and Environment Focus, 7(1), 83-89.
- Druzian, D. M., Oviedo, L. R., Loureiro, S. N., Wouters, R. D., Vizzotto, B. S., de Oliveira Pinto, E., ... & da Silva, W. L. (2023). Cerium oxide nanoparticles: Biosynthesis, characterization, antimicrobial, ecotoxicity and photocatalytic activity. Journal of Photochemistry and Photobiology A: Chemistry, 442, 114773.

- Miri, A., Beiki, H., Najafidoust, A., Khatami, M., & Sarani, M. (2021). Cerium oxide nanoparticles: green synthesis using Banana peel, cytotoxic effect, UV protection and their photocatalytic activity. Bioprocess and Biosystems Engineering, 44(9), 1891-1899.
- Elahi, B., Mirzaee, M., Darroudi, M., Oskuee, R. K., Sadri, K., & Gholami, L. (2020). Role of oxygen vacancies on photo-catalytic activities of green synthesized ceria nanoparticles in Cydonia oblonga miller seeds extract and evaluation of its cytotoxicity effects. Journal of Alloys and Compounds, 816, 152553.
- Sayed, M. A., Abo-Aly, M. M., Aziz, A. A. A., Hassan, A., & Salem, A. N. M. (2021). A facile hydrothermal synthesis of novel CeO2/CdSe and CeO2/CdTe Nanocomposites: Spectroscopic investigations for economically feasible photocatalytic degradation of Congo red dye. Inorganic Chemistry Communications, 130, 108750.
- Thomas, E., Briancon, S., Chaput, F., Magnano, G. C., Trenque, I., Arquier, D., ... & Bolzinger, M. A. (2024). Tailor-Made Synthesis of Cerium Oxide Nanoparticles for Improving the Skin Decontamination of Paraoxon. ACS Applied Nano Materials, 7(14), 16052-16065.
- Kusuma, K. B., Manju, M., Ravikumar, C. R., Raghavendra, N., Amulya, M. S., Nagaswarupa, H. P., ... & Shekhar, T. S. (2022). Photocatalytic degradation of Methylene Blue and electrochemical sensing of paracetamol using Cerium oxide nanoparticles synthesized via sonochemical route. Applied Surface Science Advances, 11, 100304.
- Jain, B., Singh, A. K., Hashmi, A., Susan, M. A. B. H., & Lellouche, J. P. (2020). Surfactant-assisted cerium oxide and its catalytic activity towards Fenton process for non-degradable dye. Advanced Composites and Hybrid Materials, 3, 430-441.
- Muthuvel, A., Jothibas, M., Mohana, V., & Manoharan, C. J. I. C. C. (2020). Green synthesis of cerium oxide nanoparticles using Calotropis procera flower extract and their photocatalytic degradation and antibacterial activity. Inorganic Chemistry Communications, 119, 108086.
- Feng KeJun, F. K., Song Biao, S. B., Li XianFeng, L. X., Liao FangLi, L. F., & Gong JiLai, G. J. (2019). Enhanced photocatalytic performance of magnetic multi-walled carbon nanotubes/cerium dioxide nanocomposite.
- Xu, T., Lei, X., Gu, G., Zou, R., & Wu, Q. (2019). Facile synthesis of CeO2-graphene oxide composites with enhanced visible-light photocatalytic performance. Materials Science and Engineering: B, 244, 49-55.
- Negi, K., Umar, A., Chauhan, M. S., & Akhtar, M. S. (2019). Ag/CeO2 nanostructured materials for enhanced photocatalytic and antibacterial applications. Ceramics International, 45(16), 20509-20517.

- Zeleke, M. A., & Kuo, D. H. (2019). Synthesis and application of V2O5-CeO2 nanocomposite catalyst for enhanced degradation of methylene blue under visible light illumination. Chemosphere, 235, 935-944.
- Li, H., Wang, G., Zhang, F., Cai, Y., Wang, Y., & Djerdj, I. (2012). Surfactant-assisted synthesis of CeO_2 nanoparticles and their application in wastewater treatment. Rsc Advances, 2(32), 12413-12423.
- Mishra, S., Soren, S., Debnath, A. K., Aswal, D. K., Das, N., & Parhi, P. (2018). Rapid microwave–Hydrothermal synthesis of CeO2 nanoparticles for simultaneous adsorption/photodegradation of organic dyes under visible light. Optik, 169, 125-136.
- Raees, A., Jamal, M. A., Ahmed, I., Silanpaa, M., & Saad Algarni, T. (2021). Synthesis and characterization of CeO2/CuO nanocomposites for photocatalytic degradation of methylene blue in visible light. Coatings, 11(3), 305.
- Krishnan, A., Vishwanathan, P. V., Mohan, A. C., Panchami, R., Viswanath, S., & Krishnan, A. V. (2021). Tuning of photocatalytic performance of CeO2-Fe2O3 composite by Sn-doping for the effective degradation of methlene blue (MB) and methyl orange (MO) dyes. Surfaces and Interfaces, 22, 100808.
- Magdalane, C. M., Kaviyarasu, K., Vijaya, J. J., Siddhardha, B., & Jeyaraj, B. (2017). Facile synthesis of heterostructured cerium oxide/yttrium oxide nanocomposite in UV light induced photocatalytic degradation and catalytic reduction: synergistic effect of antimicrobial studies. Journal of Photochemistry and Photobiology B: Biology, 173, 23-34.
- Arul, N. S., Mangalaraj, D., Chen, P. C., Ponpandian, N., Meena, P., & Masuda, Y. (2012). Enhanced photocatalytic activity of cobalt-doped CeO 2 nanorods. Journal of sol-gel science and technology, 64, 515-523.
- Saranya, J., Ranjith, K. S., Saravanan, P., Mangalaraj, D., & Kumar, R. T. R. (2014). Cobalt-doped cerium oxide nanoparticles: enhanced photocatalytic activity under UV and visible light irradiation. Materials science in semiconductor processing, 26, 218-224.
- Ahmad, T., Iqbal, J., Bustam, M. A., Zulfiqar, M., Muhammad, N., Al Hajeri, B. M., ... & Ullah, S. (2020). Phytosynthesis of cerium oxide nanoparticles and investigation of their photocatalytic potential for degradation of phenol under visible light. Journal of Molecular Structure, 1217, 128292.
- Iqbal, J., Shah, N. S., Sayed, M., Muhammad, N., Khan, J. A., Khan, Z. U. H., ... & Polychronopoulou, K. (2020). Deep eutectic solvent-mediated synthesis of ceria nanoparticles with the enhanced yield for photocatalytic degradation of flumequine under UV-C. Journal of Water Process Engineering, 33, 101012.
- Zheng, X., Huang, S., Yang, D., Zhai, H., You, Y., Fu, X., ... & Liu, Y. (2017). Synthesis of X-architecture CeO2 for the photodegradation of methylene

blue under UV-light irradiation. Journal of Alloys and Compounds, 705, 131-137. doi: 10.1016/j.jallcom.2017.02.110

- El Rouby, W. M. A., Farghali, A. A., & Hamdedein, A. (2016). Microwave synthesis of pure and doped cerium (IV) oxide (CeO2) nanoparticles for methylene blue degradation. Water Science and Technology, 74(10), 2325-2336.
- Ravishankar, T. N., Ramakrishnappa, T., Nagaraju, G., & Rajanaika, H. (2015). Synthesis and characterization of CeO2 nanoparticles via solution combustion method for photocatalytic and antibacterial activity studies. ChemistryOpen, 4(2), 146-154.
- Afza, N., Shivakumar, M. S., Alam, M. W., Kumar, A. N., Bhatt, A. S., Murthy, H. A., ... & Selvanandan, S. (2022). Facile hydrothermal synthesis of cerium oxide/rGO nanocomposite for photocatalytic and supercapacitor applications. Applied Surface Science Advances, 11, 100307.
- Ahmad, T., Iqbal, J., Bustam, M. A., Zulfiqar, M., Muhammad, N., Al Hajeri, B. M., ... & Ullah, S. (2020). Phytosynthesis of cerium oxide nanoparticles and investigation of their photocatalytic potential for degradation of phenol under visible light. Journal of Molecular Structure, 1217, 128292.
- Safat, S., Buazar, F., Albukhaty, S., & Matroodi, S. (2021). Enhanced sunlight photocatalytic activity and biosafety of marine-driven synthesized cerium oxide nanoparticles. Scientific Reports, 11(1), 14734.
- Surendra, T. V., & Roopan, S. M. (2016). Photocatalytic and antibacterial properties of phytosynthesized CeO2 NPs using Moringa oleifera peel extract. Journal of Photochemistry and Photobiology B: Biology, 161, 122-128.
- Magudieshwaran, R., Ishii, J., Raja, K. C. N., Terashima, C., Venkatachalam, R., Fujishima, A., & Pitchaimuthu, S. (2019). Green and chemical synthesized CeO2 nanoparticles for photocatalytic indoor air pollutant degradation. Materials Letters, 239, 40-44.
- Sharma, J. K., Srivastava, P., Ameen, S., Akhtar, M. S., Sengupta, S. K., & Singh, G. (2017). Phytoconstituents assisted green synthesis of cerium oxide nanoparticles for thermal decomposition and dye remediation. Materials Research Bulletin, 91, 98-107.
- Gnanam, S., Gajendiran, J., Ramya, J. R., Ramachandran, K., & Raj, S. G. (2021). Glycine-assisted hydrothermal synthesis of pure and europium doped CeO2 nanoparticles and their structural, optical, photoluminescence, photocatalytic and antibacterial properties. Chemical Physics Letters, 763, 138217.
- Magdalane, C. M., Kaviyarasu, K., Raja, A., Arularasu, M. V., Mola, G. T., Isaev, A. B., ... & Maaza, M. (2018). Photocatalytic decomposition effect of erbium doped cerium oxide nanostructures driven by visible light irradiation: investigation of cytotoxicity, antibacterial growth inhibition

using catalyst. Journal of Photochemistry and Photobiology B: Biology, 185, 275-282.

- Jayakumar, G., Irudayaraj, A. A., & Raj, A. D. (2017). Particle size effect on the properties of cerium oxide (CeO2) nanoparticles synthesized by hydrothermal method. Mechanics, Materials Science & Engineering Journal, 9(1).
- Kim, N. W., Lee, D. K., & Yu, H. (2019). Selective shape control of cerium oxide nanocrystals for photocatalytic and chemical sensing effect. RSC advances, 9(24), 13829-13837.
- Reddy Yadav, L. S., Manjunath, K., Archana, B., Madhu, C., Raja Naika, H., Nagabhushana, H., ... & Nagaraju, G. (2016). Fruit juice extract mediated synthesis of CeO 2 nanoparticles for antibacterial and photocatalytic activities. The European Physical Journal Plus, 131, 1-10.
- Zhang, M., Zhang, C., Zhai, X., Luo, F., Du, Y., & Yan, C. (2019). Antibacterial mechanism and activity of cerium oxide nanoparticles. Sci. China Mater, 62(11), 1727-1739.
- LU, X. W., QIAN, J. C., Feng, C. H. E. N., LI, X. Z., & CHEN, Z. G. (2012). Synthesis, characterization and antibacterial property of Ag/mesoporous CeO2 nanocomposite material. Transactions of Nonferrous Metals Society of China, 22(6), 1418-1422.
- Yue, L., & Zhang, X. M. (2009). Structural characterization and photocatalytic behaviors of doped CeO2 nanoparticles. Journal of Alloys and Compounds, 475(1-2), 702-705.
- Maleki, P., Nemati, F., Gholoobi, A., Hashemzadeh, A., Sabouri, Z., & Darroudi, M. (2021). Green facile synthesis of silver-doped cerium oxide nanoparticles and investigation of their cytotoxicity and antibacterial activity. Inorganic Chemistry Communications, 131, 108762.
- Balamurugan, A., Sudha, M., Surendhiran, S., Anandarasu, R., Ravikumar, S., & Khadar, Y. S. (2020). Hydrothermal synthesis of samarium (Sm) doped cerium oxide (CeO2) nanoparticles: characterization and antibacterial activity. Materials Today: Proceedings, 26, 3588-3594.
- Kannan, S. K., & Sundrarajan, M. (2014). A green approach for the synthesis of a cerium oxide nanoparticle: characterization and antibacterial activity. International journal of nanoscience, 13(03), 1450018.
- Pelletier, D. A., Suresh, A. K., Holton, G. A., McKeown, C. K., Wang, W., Gu, B., ... & Doktycz, M. J. (2010). Effects of engineered cerium oxide nanoparticles on bacterial growth and viability. Applied and environmental microbiology, 76(24), 7981-7989.
- Kareem, M. T., & Hamdan, S. A. (2024, February). Study of the influence concentration difference in properties of cerium thin films. In AIP Conference Proceedings (Vol. 2922, No. 1). AIP Publishing.

- Altaf, M., Manoharadas, S., & Zeyad, M. T. (2021). Green synthesis of cerium oxide nanoparticles using Acorus calamus extract and their antibiofilm activity against bacterial pathogens. Microscopy Research and Technique, 84(8), 1638-1648.
- Sathiyapriya, R., Balaji, M., & Rajesh, S. (2020). Bio-synthesis of cerium oxide nanoparticles from Coriandrum sativum L. leaf extract and their antibacterial activity. International Journal of Advanced Science, Engineering, 6, 1439-1444.
- Magdalane, C. M., Kaviyarasu, K., Vijaya, J. J., Siddhardha, B., & Jeyaraj, B. (2016). Photocatalytic activity of binary metal oxide nanocomposites of CeO2/CdO nanospheres: investigation of optical and antimicrobial activity. Journal of Photochemistry and Photobiology B: Biology, 163, 77-86.
- Devi, N. S., Ganapathy, D. M., Rajeshkumar, S., & Maiti, S. (2022). Characterization and antimicrobial activity of cerium oxide nanoparticles synthesized using neem and ginger. Journal of Advanced Pharmaceutical Technology & Research, 13(Suppl 2), S491-S495.
- Ahmed, H. E., Iqbal, Y., Aziz, M. H., Atif, M., Batool, Z., Hanif, A., ... & Ahmad, H. (2021). Green synthesis of CeO2 nanoparticles from the Abelmoschus esculentus extract: evaluation of antioxidant, anticancer, antibacterial, and wound-healing activities. Molecules, 26(15), 4659.
- Rahdar, A., Beyzaei, H., Askari, F., & Kyzas, G. Z. (2020). Gum-based cerium oxide nanoparticles for antimicrobial assay. Applied Physics A, 126, 1-9.
- Park, E. J., Choi, J., Park, Y. K., & Park, K. (2008). Oxidative stress induced by cerium oxide nanoparticles in cultured BEAS-2B cells. Toxicology, 245(1-2), 90-100.
- Renu, G., Rani, V. V., Nair, S. V., Subramanian, K. R. V., & Lakshmanan, V. K. (2012). Development of cerium oxide nanoparticles and its cytotoxicity in prostate cancer cells. Advanced Science Letters, 6(1), 17-25.
- Darroudi, M., Hakimi, M., Sarani, M., Oskuee, R. K., Zak, A. K., & Gholami, L. (2013). Facile synthesis, characterization, and evaluation of neurotoxicity effect of cerium oxide nanoparticles. Ceramics International, 39(6), 6917-6921.
- Bazhukova, I. N., Sokovnin, S. Y., Ilves, V. G., Myshkina, A. V., Vazirov, R. A., Pizurova, N., & Kasyanova, V. V. (2019). Luminescence and optical properties of cerium oxide nanoparticles. Optical Materials, 92, 136-142.
- Atif, M., Iqbal, S., Fakhar-e-Alam, M., Mansoor, Q., Alimgeer, K. S., Fatehmulla, A., ... & Chu, Y. M. (2021). Manganese-doped cerium oxide nanocomposite as a therapeutic agent for MCF-7 adenocarcinoma cell line. Saudi Journal of Biological Sciences, 28(2), 1233-1238.
- Abbas, F., Jan, T., Iqbal, J., Naqvi, M. S. H., & Ahmad, I. (2016). Inhibition of Neuroblastoma cancer cells viability by ferromagnetic Mn doped CeO2

monodisperse nanoparticles mediated through reactive oxygen species. Materials Chemistry and Physics, 173, 146-151.

- Abbas, F., Iqbal, J., Maqbool, Q., Jan, T., Ullah, M. O., Nawaz, B., ... & Ahmad, I. (2017). ROS mediated malignancy cure performance of morphological, optical, and electrically tuned Sn doped CeO2 nanostructures. AIP Advances, 7(9).
- Abbas, F., Jan, T., Iqbal, J., Ahmad, I., Naqvi, M. S. H., & Malik, M. (2015). Facile synthesis of ferromagnetic Ni doped CeO2 nanoparticles with enhanced anticancer activity. Applied Surface Science, 357, 931-936.
- Lin, Y. H., Shen, L. J., Chou, T. H., & Shih, Y. H. (2021). Synthesis, stability, and cytotoxicity of novel cerium oxide nanoparticles for biomedical applications. Journal of Cluster Science, 32, 405-413.
- Miri, A., & Sarani, M. (2018). Biosynthesis, characterization and cytotoxic activity of CeO2 nanoparticles. Ceramics International, 44(11), 12642-12647.
- Miri, A., Darroudi, M., & Sarani, M. (2020). Biosynthesis of cerium oxide nanoparticles and its cytotoxicity survey against colon cancer cell line. Applied Organometallic Chemistry, 34(1), e5308.
- Kargar, H., Ghazavi, H., & Darroudi, M. (2015). Size-controlled and bio-directed synthesis of ceria nanopowders and their in vitro cytotoxicity effects. Ceramics International, 41(3), 4123-4128.
- Zhong, L. S., Hu, J. S., Cao, A. M., Liu, Q., Song, W. G., & Wan, L. J. (2007). 3D flowerlike ceria micro/nanocomposite structure and its application for water treatment and CO removal. Chemistry of Materials, 19(7), 1648-1655.
- Nourmohammadi, E., Oskuee, R. K., Hasanzadeh, L., Mohajeri, M., Hashemzadeh, A., Rezayi, M., & Darroudi, M. (2018). Cytotoxic activity of greener synthesis of cerium oxide nanoparticles using carrageenan towards a WEHI 164 cancer cell line. Ceramics International, 44(16), 19570-19575.
- Ashna, M., Es-Haghi, A., Karimi Noghondar, M., Al Amara, D., & Yazdi, M. E. T. (2022). Greener synthesis of cerium oxide nanoemulsion using pollen grains of Brassica napus and evaluation of its antitumour and cytotoxicity properties. Materials Technology, 37(8), 525-532.
- Javadi, F., Yazdi, M. E. T., Baghani, M., & Es-haghi, A. (2019). Biosynthesis, characterization of cerium oxide nanoparticles using Ceratonia siliqua and evaluation of antioxidant and cytotoxicity activities. Materials Research Express, 6(6), 065408.
- Sridharan, M., Kamaraj, P., Arockiaselvi, J., Pushpamalini, T., Vivekanand, P. A., & Kumar, S. H. (2021). Synthesis, characterization and evaluation of biosynthesized Cerium oxide nanoparticle for its anticancer activity on breast cancer cell (MCF 7). Materials Today: Proceedings, 36, 914-919.

- Abbasi, N., Homayouni Tabrizi, M., Ardalan, T., & Roumi, S. (2022). Cerium oxide nanoparticles-loaded on chitosan for the investigation of anticancer properties. Materials Technology, 37(10), 1439-1449.
- Kermani, G., Karimi, E., & Tabrizi, M. H. (2022). Hybrid nanoarchitectonics of chitosan-cerium oxide nanoparticles for anticancer potentials. Journal of Inorganic and Organometallic Polymers and Materials, 32(7), 2591-2599.
- Schubert, D., Dargusch, R., Raitano, J., & Chan, S. W. (2006). Cerium and yttrium oxide nanoparticles are neuroprotective. Biochemical and biophysical research communications, 342(1), 86-91.
- Zholobak, N. M., Shcherbakov, A. B., Ivanova, O. S., Reukov, V., Baranchikov, A. E., & Ivanov, V. K. (2020). Nanoceria-curcumin conjugate: Synthesis and selective cytotoxicity against cancer cells under oxidative stress conditions. Journal of Photochemistry and Photobiology B: Biology, 209, 111921.
- Parvathya, S., & Venkatramanb, B. R. (2017). In vitro antibacterial and anticancer potential of CeO2 nanoparticles prepared by co-precipitation and green synthesis method. J. Nanosci. Curr. Res, 2(02), 1-9.
- Ganeshkar, M. P., Goder, P. H., Mirjankar, M. R., Gaddigal, A. T., Shivappa, P., & Kamanavalli, C. M. (2024). Characterization and screening of anticancer properties of cerium oxide nanoparticles synthesized using Averrhoa carambola plant extract. Inorganic and Nano-Metal Chemistry, 54(8), 779-792.
- Nazaripour, E., Mousazadeh, F., Moghadam, M. D., Najafi, K., Borhani, F., Sarani, M., ... & Khatami, M. (2021). Biosynthesis of lead oxide and cerium oxide nanoparticles and their cytotoxic activities against colon cancer cell line. Inorganic Chemistry Communications, 131, 108800.
- Hamidian, K., Saberian, M. R., Miri, A., Sharifi, F., & Sarani, M. (2021). Doped and un-doped cerium oxide nanoparticles: Biosynthesis, characterization, and cytotoxic study. Ceramics International, 47(10), 13895-13902.
- Alghamdi, A. A. (2023). Biogenic Mg doped CeO2 nanoparticles via Hibiscus sabdariffa and its potential biological applications. Journal of Umm Al-Qura University for Applied Sciences, 9(2), 132-141.
- Taherzadeh, D., Amiri, H., Ebrahimi, S., Ghafarpour, A., Samandarinejad, N., Darroudi, M., & Hashemy, S. I. (2023). Green synthesis of cerium oxide nanoparticles using Falcaria Vulgaris leaf extract and its anti-tumoral effects in prostate cancer.
- Nourmohammadi, E., Oskuee, R. K., Hasanzadeh, L., Mohajeri, M., Hashemzadeh, A., Rezayi, M., & Darroudi, M. (2018). Cytotoxic activity of greener synthesis of cerium oxide nanoparticles using carrageenan towards a WEHI 164 cancer cell line. Ceramics International, 44(16), 19570-19575.

- Soren, S., Jena, S. R., Samanta, L., & Parhi, P. (2015). Antioxidant potential and toxicity study of the cerium oxide nanoparticles synthesized by microwave-mediated synthesis. Applied biochemistry and biotechnology, 177, 148-161.
- Hirst, S. M., Karakoti, A. S., Tyler, R. D., Sriranganathan, N., Seal, S., & Reilly, C. M. (2009). Anti-inflammatory properties of cerium oxide nanoparticles. Small, 5(24), 2848-2856.
- Patil, S. N., Paradeshi, J. S., Chaudhari, P. B., Mishra, S. J., & Chaudhari, B. L. (2016). Bio-therapeutic potential and cytotoxicity assessment of pectin-mediated synthesized nanostructured cerium oxide. Applied Biochemistry and Biotechnology, 180, 638-654.
- Shlapa, Y., Solopan, S., Sarnatskaya, V., Siposova, K., Garcarova, I., Veltruska, K., ... & Belous, A. (2022). Cerium dioxide nanoparticles synthesized via precipitation at constant pH: Synthesis, physical-chemical and antioxidant properties. Colloids and Surfaces B: Biointerfaces, 220, 112960.
- Chaudhary, R. G., Chouke, P. B., Bagade, R. D., Potbhare, A. K., & Dadure, K. M. (2020). Molecular docking and antioxidant activity of Cleome simplicifolia assisted synthesis of cerium oxide nanoparticles. Materials Today: Proceedings, 29, 1085-1090.
- Gallucci, N., Vitiello, G., Di Girolamo, R., Imbimbo, P., Monti, D. M., Tarallo, O., ... & Paduano, L. (2021). Towards the development of antioxidant cerium oxide nanoparticles for biomedical applications: Controlling the properties by tuning synthesis conditions. Nanomaterials, 11(2), 542.
- Singh, S., Kumar, U., Gittess, D., Sakthivel, T. S., Babu, B., & Seal, S. (2021). Cerium oxide nanomaterial with dual antioxidative scavenging potential: Synthesis and characterization. Journal of Biomaterials Applications, 36(5), 834-842.
- Dutta, D., Mukherjee, R., Ghosh, S., Patra, M., Mukherjee, M., & Basu, T. (2022). Cerium oxide nanoparticles as antioxidant or pro-oxidant agents. ACS Applied Nano Materials, 5(1), 1690-1701.